LBL-26164
Preprint

Lawrence Berkeley Laboratory
UNIVERSITY OF CALIFORNIA

RECEIVED
BERKELEY LABORATORY
SEP 14 1989
LIBRARY AND
DOCUMENTS SECTION

Submitted to Nuclear Physics A

Theory of Nuclear Multifragmentation
I. Transition-State Treatment of the Breakup Process

J.A. López and J. Randrup

April 1989

TWO-WEEK LOAN COPY
This is a Library Circulating Copy
which may be borrowed for two weeks.

NUCLEAR SCIENCE DIVISION

LBL-26164 c.2

Prepared for the U.S. Department of Energy under Contract Number DE-AC03-76SF00098.

DISCLAIMER

This document was prepared as an account of work sponsored by the United States Government. While this document is believed to contain correct information, neither the United States Government nor any agency thereof, nor the Regents of the University of California, nor any of their employees, makes any warranty, express or implied, or assumes any legal responsibility for the accuracy, completeness, or usefulness of any information, apparatus, product, or process disclosed, or represents that its use would not infringe privately owned rights. Reference herein to any specific commercial product, process, or service by its trade name, trademark, manufacturer, or otherwise, does not necessarily constitute or imply its endorsement, recommendation, or favoring by the United States Government or any agency thereof, or the Regents of the University of California. The views and opinions of authors expressed herein do not necessarily state or reflect those of the United States Government or any agency thereof or the Regents of the University of California.

LBL-26164

Theory of Nuclear Multifragmentation
I. Transition-State Treatment of the Breakup Process

Jorge A. López and Jørgen Randrup

Nuclear Science Division, Lawrence Berkeley Laboratory
University of California, Berkeley, California 94720

April 30, 1989

Abstract:

The transition-state treatment of ordinary binary fission is generalized to describe statistical disassembly of a highly excited nucleus into multifragment channels. In this first part of the work, the focus is on deriving the general expressions for the transition widths into an assembly of specified prefragments. These are still interacting and may experience a significant post-transition evolution which will be addressed in part II of this work. The transition configurations are described in terms of a number of interacting prefragments, whose positions are constrained by a generalized disassembly degree of freedom characterizing the overall spatial extension of the system and whose phase space is included in the statistical weight. Angular-momentum conservation is readily incorporated in the formulation. The treatment is discussed in relation to standard fission theory and statistical multifragmentation models.

*This work was supported in part by the Director, Office of Energy Research, Office of High Energy and Nuclear Physics, Division of High Energy Physics, of the U.S. Department of Energy under Contract No. DE-AC03-76SF00098.

Contents

1 Introduction **1**
- 1.1 Standard treatment of fission . . . 1
- 1.2 Extension to multifragmentation . . . 4

2 Description of the disassembling system **5**
- 2.1 Multifragment systems . . . 6

3 Transition-state treatment **8**
- 3.1 Disassembly variables . . . 8
- 3.2 Density of states . . . 10
- 3.3 Transition current . . . 12
- 3.4 Breakup width . . . 13

4 Discussion **13**
- 4.1 The location of the transition surface . . . 14
- 4.2 The choice of disassembly coordinate . . . 14
- 4.3 Correction for misalignment . . . 15
- 4.4 Binary fission . . . 16
- 4.5 Statistical multifragmentation . . . 17
- 4.6 Evolution of prefragment multiplicity with energy . . . 19

5 Concluding remarks **20**

A Potential energy **21**

B Internal level density **24**
- B.1 Integration over internal excitation . . . 25

C Condensed multifragment notation **26**

D Microcanonical phase space **28**
- D.1 Energy conservation . . . 28
- D.2 Energy and momentum conservation . . . 28
- D.3 Conservation of energy, momentum, and outwards flow . . . 29
- D.4 Constrained positions . . . 31

E Angular momentum **31**
- E.1 Nuclear level density . . . 31
- E.2 Multifragment system . . . 32
- E.3 Binary system . . . 34

1 Introduction

Multifragmentation processes are presently of central interest in nuclear physics. The experimental basis for this topic is the fact that highly excited nuclear systems can be produced in the laboratory by use of medium-energy heavy-ion beams (or high-energy protons); these systems typically disassemble into several, or many, (moderately excited) nuclear fragments. Such multifragmentation processes are not yet well understood, in spite of vigorous efforts, both experimental and theoretical.

For the nuclear multifragmentation problem, several statistical models have been developed in recent years, based on excitable fragments within a specified freeze-out volume.[1,2,3,4] Such a scenario is of direct relevance to the study of dilute nuclear matter (at not too high temperatures) and the formulation of the associated statistical mechanics is relatively straightforward, even when fragment interactions are incorporated.[2] Application of such statistical models to the disassembly of a nuclear "source" (an idealization of the transient excited system produced in an energetic nuclear collision) has usually been made by simply assuming that the yield of a given final channel is proportional to the corresponding statistical weight. This type of approach can be viewed as a rather crude transition-state approximation.

Although capable of reproducing a variety of features of the data, such approaches are not entirely satisfactory. A principal problem is that there is no inherent way of determining the freeze-out volume, which therefore must be prescribed by some argument external to the model, or perhaps fitted to data. A related problem is that the potential barriers are not given appropriate consideration (even if fragment interactions are incorporated in the calculation of the statistical weight for a given configuration, as in [2]). Experience from binary fission has shown that the potential-energy barriers have a controlling influence on the decay widths. Moreover, the propagation of the fragmenting system from the freeze-out configuration to asymptotia is dependent on how the potential energy is treated. These problems are particularly serious at relatively moderate excitations and they need to be adequately solved before it is possible to clarify such key questions as the transition from the ordinary sequential-binary type of decay characteristic of low excitation to the nearly simultaneous multifragment breakup apparently occurring at high excitation.

This unsatisfactory situation has motivated us to formulate a refined treatment of statistical multifragmentation based on a suitable generalization of the transition-state approximation for ordinary binary fission. Before embarking on the formal developments, the standard treatment is briefly reviewed, in order to provide an instructive background for our discussion, and our generalized treatment is briefly summarized.

1.1 Standard treatment of fission

The transition-state method commonly used to study binary fission was adapted by Bohr and Wheeler in 1939[5], the year nuclear fission was discovered, now fifty

years ago. This treatment estimates the number of fission events per unit time by considering a statistical ensemble of similarly prepared excited nuclei and counting how many of them traverse the transition state per unit time. Although the method was formulated for symmetric fission, for which there is a well-defined saddle shape, it can be generalized to asymmetric splits as well, by considering the appropriate conditional saddles.

The treatment can be briefly described as follows. We wish to calculate the rate at which an excited compound nucleus with mass number A and total energy E fissions into two fragments with given mass numbers, A_1 and A_2. If the ground-state energy of the decaying nucleus is denoted by E_0, its excitation energy is $\epsilon_0 = E - E_0$. The corresponding total density of states for the compound system, $\rho_A(\epsilon_0)$, is often approximated by a simple Fermi-gas level density. The fission process can be visualized as a diffusive evolution of the nuclear shape, starting at the spherical ground state, where the statistical weight is concentrated, and ultimately developing into two receding fragments with the specified mass numbers. Although the nucleus in general explores a multidimensional space of shapes, it is convenient to consider a one-dimensional sequence of shapes, as can be determined by considering the path of least action through the multidimensional space of nuclear shapes, for example. Let the associated macroscopic degree of freedom be denoted q, the fission degree of freedom. Let the conjugate fission momentum be denoted p and let the associated effective inertial mass be μ. The kinetic energy of the collective fission motion is then $k = p^2/2\mu$. [It should be noted that the description in terms of the fission variables (q, p) is only needed in the neighborhood of the transition configuration.]

The specification of the fission variables (q, p) presents a macroscopic constraint on the system and the amount of energy left for sharing between the remaining degrees of freedom is given by $E^\star = E - E_{12}^0 - V(q) - k$. Here $E_{12}^0 \equiv E_1^0 + E_2^0$ is the sum of the ground-state energies of the two fission fragments and $V(q)$ represents the potential energy of deformation implied by the specified value of q. In order to conform with our later formulation, the reference energy is chosen such that $V(q)$ reduces to the interaction energy between the receding fragments for large values of q; the ordinary deformation energy is then given by $E_{\rm def}(q) = E_{12}^0 - E_0 + V(q)$. For naturally occurring nuclei, this deformation energy exhibits a maximum as q is increased, thus defining the (conditional) fission barrier.

The constrained system is referred to as the "activated complex" and its density of states is $\rho_{12}^\star(E; q, p)$. This quantity represents the statistical weight for finding the considered system with the specified values (q, p). The activated complex is regarded as a deformed manifestation of the decaying compound nucleus, with a shape determined by the specified masses A_1 and A_2, and the specified value of the fission coordinate q. The density of internal states for such a dinucleus is conveniently denoted by $\rho_{12}(\epsilon)$, where ϵ is the internal excitation energy. Ordinarily, the level density of the activated complex $\rho_{12}^\star(E; q, p)$ is taken to be equal to the internal level density $\rho_{12}(\epsilon)$. This simplest view ignores any additional collective degrees of freedom associated with the activated complex, in particular the individual trans-

lational and rotational motion of the two binary parts that would be possible for a dispherical system. Our later discussions will further clarify the distinction between the internal level density $\rho_{12}(\epsilon)$ and the level density $\rho^{\star}_{12}(E;q,p)$ for the activated complex.

The outwards directed probability flow at any specified value of q is given by

$$\begin{aligned} \nu_{A_1A_2}(E) &= \int \frac{dp}{h}\,\frac{p}{\mu}\,\rho^{\star}_{12}(E;q,p) = \frac{1}{h}\int dk\;\rho_{12}(E-E^0_{12}-V(q)-k) \\ &= \frac{1}{h}\int_0^{\epsilon_{12}} d\epsilon\;\rho_{12}(\epsilon)\;\approx\;\frac{1}{h}\;\rho_{12}(\epsilon_{12})\;\tau_{12}\;, \end{aligned} \tag{1}$$

where the maximum internal excitation energy of the activated complex is $\epsilon_{12} = E - E^0_{12} - V(q_{12})$. The flux factor p/μ is the velocity of the fission motion and can be seen as the result of a local integration over those values of q passing by the specified point during an infinitesimal time interval. The last relation results from a first-order logarithmic expansion of the integrand around ϵ_{12} and the internal temperature τ_{12} is given by the inverse of $\partial \ln \rho_{12}(\epsilon)/\partial\epsilon$ evaluated at $\epsilon = \epsilon_{12}$.

Considered as a function of q, the above flux (1) exhibits a minimum at the fission barrier, where ϵ_{12} is the smallest. The corresponding value of the fission coordinate is then taken to characterize the fission transition state. It may be denoted by q_{12} to remind of the fact that it depends on the particular mass partition A_1A_2 considered. The corresponding fission decay rate t^{-1}_{12} is then obtained as the above current (1) divided by $\rho_A(\epsilon_0)$. This latter quantity, the total density of states for the compound nucleus, represents the total number of states with nuclear shapes that are more compact than the transition shape, *i.e.* have $q < q_{12}$. Consequently, the decay width for fission into the specified mass partition can be written in the simple form

$$\begin{aligned} \Gamma_{A_1A_2}(E) \equiv \frac{h}{t_{12}} &= \frac{1}{h}\,\frac{\nu_{A_1A_2}(E)}{\rho_A(\epsilon_0)} \\ &= \frac{1}{\rho_A(\epsilon_0)}\int_0^{\epsilon_{12}} d\epsilon\;\rho_{12}(\epsilon)\;\approx\;\frac{\rho_{12}(\epsilon_{12})}{\rho_A(\epsilon_0)}\;\tau_{12}\;. \end{aligned} \tag{2}$$

As pointed out by Swiatecki[6], this expression is globally applicable to *all* binary mass partitions, including light-particle evaporation and is therefore well-suited for studying the competition between ordinary near-symmetric fission and the very asymmetric light-particle emission.

The above treatment singles out one collective degree of freedom, q, and assumes that all other degrees of freedom maintain statistical equilibrium up to the transition point, at which point they are "frozen". This is of course a drastic simplification of the complicated (and interesting) dynamics taking place. In actuality more than one collective degree of freedom may be important and they generally freeze out of different stages of the fission process. Nevertheless, the simple transition-state approximation, as represented by (2), has proven to be very useful for understanding general features of the fission process.

It should also be noted that the resulting formula (2) does not depend on the specific choice of fission coordinate: any shape parametrization leading though the conditional saddle point will yield that same result. [This simple and convenient feature also brings out a shortcoming of the formula (2), namely that it is insensitive to the stiffness of the saddle in the direction(s) perpendicular to the fission direction.]

1.2 Extension to multifragmentation

When the compound system disassembles into several fragments, the identification of a single "fission" degree of freedom is not so obvious and, moreover, the assumption of simultaneous freeze-out of all collective degrees of freedom appears even less justified. Nevertheless, the development of a transition-state treatment of multiple fission is a worthwhile undertaking, since it will provide a relatively simple and global means for exploring general features of such processes.

A first step is to develop a formal framework for treating the disassembling system. For this we describe the system in terms of the degrees of freedom associated with a (variable) number of interacting (pre)fragments, as is ordinarily done in current multifragmentation models. This basic formalism is presented and discussed in Section 2.

Then, in Section 3, we introduce a generalized fission degree of freedom q in terms of the overall size of the system; its conjugate momentum p is a measure of the outwards directed flow in the system. The statistical weight of a specified set of disassembly variables (q, p) can then be calculated as the sum over all multifragment states compatible with those values. This can be done for any particular mass partition $A_1, ..., A_N$ and conservation of overall mass, energy, momentum, and position is ensured. Conservation of overall angular momentum can also be incorporated without essential complication.

The generalized fission variables (q, p) can be considered for any particular relative arrangement of the fragments and are then associated with a simple scaling of the relative positions of the fragments. Considered as a function of the scaling variable, the outwards probability current can be expressed in terms of the internal level density of the multifragment system, in analogy with the simple binary case reviewed above, and its minimum determines the transition state. Because the phase space associated with the fragment positions grows with the volume, the transition state generally lies (slightly) inside the maximum in the potential energy.

The width $\Gamma_{A_1 \cdots A_N}(E)$ for disassembly into the specified mass partition can then be calculated in terms of the probability current at the transition point, in complete analogy with the standard treatment. The resulting expression for Γ involves an average over the relative positions of the N prefragments and must be evaluated by a numerical Monte-Carlo sampling, due to the complicated dependence of the potential energy on the prefragment positions and the large number of contributing configurations. Nevertheless, the treatment is no more demanding than current statistical models for multifragmentation.

The resulting formulation is discussed in Section 4. At low excitations, where binary decay channels dominate, it is of interest to compare with the standard treatment described above; though very similar to (2), our result has an extra factor related to the relative orbital motion of the two fragments. At high excitation our treatment is rather similar to standard statistical multifragmentation models, but some notable differences are present, due to the fact that our decay rate is determined by the transition *flux*, rather than the statistical *weight*. An important feature of our formulation is that the "freeze-out volume" is not a prescribed or adjustable quantity but is determined within the model itself.

An important feature of our present treatment of multifragmentation is that the transition-state formula gives the width $\Gamma_{A_1 \cdots A_N}(E)$ for disassembly into N *pre*fragments which are still subject to considerable mutual interaction. In fact the post-transition evolution of the system is expected to have a significant effect on the final channel and it is necessary to take this stage of the disassembly process into account when seeking to calculate observable quantities, such as the fragment mass distribution. The significance of the post-transition dynamics is an important feature that complicates the treatment of multiple breakup relative to binary fission. We plan to address this essential part of the problem in a subsequent paper[7].

Our concluding remarks are made in Section 5. In Appendix A we describe our preliminary method for evaluating the potential energy of a multifragment system as a function of its spatial configuration and in Appendix B we discuss the internal level density. In Appendix C we present a condensed notation which can be convenient in the discussion of multifragment systems. Appendix D contains the analytical evaluation of various constrained integrals needed in the formal developments. Finally, in Appendix E we address the question of angular-momentum conservation and show how that aspect is easily incorporated into our formulation.

2 Description of the disassembling system

The present work seeks to develop a theory for the disassembly of a very excited nucleus into a number of fragments. The main task will be to characterize the "transition state", *i.e.* the configuration (or configuration class, rather) at which the system undergoes an irreversible transformation into interacting prefragments.

We shall assume that this transition configuration bears some resemblance to a collection of the specified prefragments, just as the ordinary fission saddle shape resembles the final channel by way of having a binary appearance and a fairly well-defined mass asymmetry. For binary fission of relatively light systems the prefragments at the saddle are fairly well developed and it is natural to describe the fissioning complex in terms of the degrees of freedom associated with a dinucleus, *i.e.* two individual nuclei with a suitable interaction potential. Even for binary fission of very heavy nuclei, for which the saddle shapes are rather compact (because the electrostatic repulsion grows stronger), such a description can be maintained, as we shall show below. We have found that for multiple breakup the prefragments

of the relevant transition configurations are in fact fairly well developed (see Appendix A), so it is quite reasonable to employ a parametrization in terms of distinct prefragments, with a suitable interaction potential.

We therefore describe the disassembling system as a collection of a (variable) number of interacting (pre)fragments. [Henceforth we shall, for brevity, usually refer to these as merely fragments, rather than the more cumbersome term prefragments; but it should be kept in mind that these fragments are subject to significant post-transition evolution not considered in the present work.] In this manner, the degrees of freedom associated with a given final channel are included explicitly already at the transition stage, even though the fragments may not yet have been fully developed as separate entities. The general formalism is then quite similar to that employed in current statistical multifragmentation models, which is very convenient.

As in the binary case, a central problem associated with such a formulation is the construction of a suitable potential energy function in terms of the spatial configuration of the prefragments. The internal level density must also be carefully modified to take account of the particular "shape" of the transition configuration. These ingredients are described further in Appendices A and B, respectively. Although they are quantitatively important, the general formulation of our treatment does not depend on their specific forms, in the same manner as the Bohr-Wheeler treatment is independent of what particular models are used for calculating the barriers and the level densities.

2.1 Multifragment systems

The formulation of the statistical mechanics for nuclear multifragment systems given in ref. [2] presents a convenient starting point for our formal developments. In that treatment the system considered appears as a (variable) number of distinct (but interacting) fragments. Any such manifestation of the system is called a *fragmentation* and is denoted by F,

$$F \; : \; \{A_n, \; \mathbf{r}_n, \; \mathbf{p}_n, \; \epsilon_n, \; n = 1, ..., N_F\} \; . \tag{3}$$

Thus, there are N_F fragments and A_n, $\mathbf{r}_n$, $\mathbf{p}_n$, ϵ_n denote the mass number, position, momentum, and internal excitation energy of fragment n, respectively.

For a system with mass number A and energy E the microcanonical density of states can be written

$$\rho(A, E) \equiv h^3 \frac{dN_A(E)}{d\mathbf{R}\; d\mathbf{P}\; dE} = h^3 \sum_F \delta(A_F - A)\; \delta(E_F - E)\; \delta(\mathbf{P}_F - \mathbf{P})\; \delta(\mathbf{R}_F - \mathbf{R}) \; , \tag{4}$$

where $\mathbf{R}_F = \frac{1}{m_0} \sum_n m_n \mathbf{r}_n$ is the overall center-of-mass position and $\mathbf{P}_F = \sum_n \mathbf{p}_n$ is the total momentum. For convenience, we shall henceforth work in the CM reference frame, where both $\mathbf{R}$ and $\mathbf{P}$ vanish. Furthermore, $A_F = \sum_n A_n$ is the total mass number of the particular fragmentation, and E_F is its total energy. This latter

quantity is assumed to be of the form

$$\begin{aligned} E_F &= \sum_{n=1}^{N_F}(E_n^0 + \epsilon_n + \frac{p_n^2}{2m_n}) + V(\mathbf{r}_1, ..., \mathbf{r}_N) \\ &= E_{1...N}^0 + \epsilon + E_{\text{kin}} + V \ . \end{aligned} \tag{5}$$

Here $E_{1...N}^0 = \sum_n E_n^0$ is the sum of the ground-state energies of the N fragments, and $\epsilon = \sum_n \epsilon_n$ is their total internal excitation energy. The total kinetic energy of the fragments is $E_{\text{kin}} = \sum_n p_n^2/2m_n$, where the inertial mass m_n is approximately equal to A_n times the nucleon mass. It is furthermore assumed that the potential energy V depends only on the fragment positions.

The multiplication by the factor h^3 in (4) has been made to conform with the usual convention for the level density $\rho(A, E)$. To be precise, the level density $\rho(A, E)$ is the number of states for the system having an energy in the specified energy interval dE, when the variables $\mathbf{R}_F$ and $\mathbf{P}_F$ describing its center of mass are constrained to be within a phase-space volume of h^3.

It should be noted that the above expression (4) for the level density ignores the conservation of total angular momentum. This simplification has been made for convenience and introduces some inaccuracy into the resulting formulas. In Appendix E we discuss this aspect and show how angular-momentum conservation can be readily incorporated into our formulation, without introducing any essential complication.

It is convenient to decompose the total density of states (4) according to mass partition $A_1, ..., A_N$,

$$h^{-3}\rho(A, E) = \frac{dN_A(E)}{d\mathbf{R}\ d\mathbf{P}\ dE} = \frac{1}{N!}\sum_N \prod_{n=1}^N \left[\sum_{A_n}\right] \delta(\sum_{n=1}^N A_n - A)\ \frac{dN_{A_1...A_N}(E)}{d\mathbf{R}\ d\mathbf{P}\ dE} \ . \tag{6}$$

The division by $N!$ compensates for the fact that the summation over fragment mass numbers produces $N!$ terms for which the fragment masses only differ by the order of their labelling. In the above decomposition, the contribution to the density of states from a particular mass partition is given by

$$\frac{dN_{A_1...A_N}(E)}{d\mathbf{R}\ d\mathbf{P}\ dE} = \prod_{n=1}^N \left[\int \frac{d\mathbf{r}_n d\mathbf{p}_n}{h^3} \int d\epsilon_n\ \rho_n(\epsilon_n)\right] \delta(E_F - E)\ \delta(\mathbf{P}_F)\ \delta(\mathbf{R}_F)\ , \tag{7}$$

where $\rho_n(\epsilon_n)$ is the internal level density for fragment n.

It is important to note that although the above decomposition (7) of the compound level density is formally correct, it has two significant problems. The first is the practical problem associated with the fact that the parametrization of the system in terms of a number of distinct prefragments grows increasingly obscure as the configuration considered becomes more compact. Since most of the statistical weight arises from rather compact configurations, this problem renders the above expression unreliable for calculating the total level density of the system. However, for the transitional configurations of primary interest in the present work, the description in terms of interacting fragments appears more reasonable.

The second problem with the expression (7) is the fact that each of the terms are ill-defined since they arise from an unbounded integration over the fragment positions. Although this is a general problem, it is usually of little importance since the nature of the system may readily suggest how to truncate the position integrals. For example, in ordinary compound nuclei each binary fission channel has an associated potential barrier (where the statistical weight has a minimum) and it is natural to define the compound nucleus as comprising all states lying inside of the fission barrier. A similar approach can be taken in the present case and (7) can be expressed in terms of an integration over the fission coordinate q (to be defined in (9)). A well-defined compound-nuclear level density can then be obtained by extending the q-integration up to the value for which the integrand has its minimum.

Fortunately, the problems associated with calculating the level density of the disassembling system are not central to our present undertaking which is focussed on developing the transition-state formulation. In our illustrative applications, we shall usually employ standard expressions for the compound nuclear level density (see Appendix B), as would be accurate at relatively low excitations where the dominant contribution to the statistical weight comes from compact configurations. At higher excitations, however, the disassembling system is often found in fragmented configurations and the standard level-density expression will significantly underestimate the level density. In such a situation it is preferable to concentrate on the branching ratios, rather than the absolute decay widths.

3 Transition-state treatment

In the following, we shall concentrate on the breakup into a specified mass partition $A_1, ..., A_N$ and derive a transition-state expression for the corresponding partial width $\Gamma_{A_1 \cdots A_N}(E)$. The total width $\Gamma_A^N(E)$ for breakup into any N prefragments can then be obtained by performing a summation over the various contributing mass partitions,

$$\Gamma_A^N(E) = \frac{1}{N!} \prod_{n=1}^{N} \left[\sum_{A_n} \right] \delta(\sum_{n=1}^{N} A_n - A) \, \Gamma_{A_1 \cdots A_N}(E) \, , \tag{8}$$

and the total breakup width is $\Gamma_A^{\text{total}}(E) = \sum_n \Gamma_A^N(E)$. As already emphasized, the disassembling system is expected to experience significant further development subsequent to the breakup transition into interacting prefragments and this feature must be taken into account before observable quantities can be calculated; we shall address this problem in a subsequent paper[7].

3.1 Disassembly variables

As already noted, in order for the density of states (7) to yield a finite result, the fragment positions must be somehow confined. This is ordinarily accomplished by

requiring the fragment positions to be within a specified volume Ω. While such a scenario is appropriate for studies of infinite matter, which can be approximated by periodic boundary conditions, the nature of the confining agency is less obvious for an isolated finite system, such as may be formed in a nuclear collision. In our present treatment, we shall replace the somewhat artificial volume Ω by a suitable generalized fission (or disassembly) coordinate whose function is to constrain the overall spatial extension of the multifragment system so that the position integrals remain convergent. The corresponding density of states is well-defined and can be considered as a function of the disassembly variable. In this manner the breakup problem can be reduced to a one-dimensional form and is then amenable to a transition-state treatment in analogy with ordinary binary fission.

Towards this end we define, for a given fragmentation F, the disassembly coordinate q and its conjugate momentum p as follows,

$$q_F^2 = \frac{1}{m_0}\sum_{n=1}^{N} m_n r_n^2 , \tag{9}$$

$$p_F = \frac{1}{q_F}\sum_{n=1}^{N} \mathbf{p}_n \cdot \mathbf{r}_n , \tag{10}$$

Thus, these variables represent the radial position and momentum in hyperspace. It then follows that q and p are conjugate variables, as is elementary to verify by evaluating their Poisson bracket,

$$\{q,p\} = \sum_n [\frac{\partial q}{\partial \mathbf{r}_n}\cdot\frac{\partial p}{\partial \mathbf{p}_n} - \frac{\partial q}{\partial \mathbf{p}_n}\cdot\frac{\partial p}{\partial \mathbf{r}_n}] = \sum_n \frac{1}{2q} 2m_n \mathbf{r}_n \cdot \mathbf{r}_n \frac{1}{q} = 1 . \tag{11}$$

Furthermore, the associated inertial mass is given by $m_0 = \sum_n m_n$, since the kinetic energy in the disassembly degree of freedom is $k = \frac{1}{2}p\dot{q} = p^2/2m_0$. The quantity q is simply related to the *rms* radius of the total thus system and provides a general and convenient measure of the overall linear dimension of the multifragment system. Its conjugate momentum p is a simple measure of the outwards directed momentum of the fragments (the "radial flow").

It might be noted that the variables q and p have vanishing Poisson brackets with the CM position $\mathbf{R}$ and the CM momentum $\mathbf{P}$, provided the configuration considered are restricted to the hypersurface characterized by $\mathbf{R}$=$\mathbf{0}$, $\mathbf{P}$=$\mathbf{0}$, as those of present interest do. If more general configurations are considered, the definition of q and p should be modified by the replacements $\mathbf{r}_n \to \mathbf{r}_n - \mathbf{R}$ and $\mathbf{p}_n \to \mathbf{p}_n - \mathbf{P}$, in order to ensure the vanishing of $\{q,\mathbf{R}\}$, $\{q,\mathbf{P}\}$, $\{p,\mathbf{R}\}$, and $\{p,\mathbf{P}\}$.

There are $3N$ degrees of freedom associated with the positions of the N fragments. Three of these are associated with an overall translation. Furthermore, the variables q and p introduced above are associated with an overall rescaling of the fragment positions. The remaining $3N$-4 positional degrees of freedom can be regarded as generalized angular variables (see Appendix C). Three of these degrees of freedom can be chosen as the usual Euler angles (ϕ,θ,ψ) describing the overall spatial orientation of the system, with the rest describing the relative locations of

the fragments (the "shape"), for given values of the CM position $\mathbf{R}_F$, the size q, and the orientation (as defined by means of the overall inertial tensor, for example).

3.2 Density of states

The variables q and p are easily introduced into the formulation by applying the identity operation $\int dqdp\ \delta(q_F - q)\delta(p_F - p)$ to the expression (7) for the density of states for the particular mass partition considered. The density of states can then be considered as a function of q and p, and a transition-state formulation very similar to the Bohr-Wheeler treatment can be readily made. However, this avenue would lead to a rather crude description, because the properties of the transition configuration are expected to vary significantly with the relative positions of the fragments, *i.e.* the angular variables in the position hyperspace. A more refined formulation can be obtained by employing q and p as local (rather than global) variables. This can be achieved by reversing the order of integration and thus consider

$$\begin{aligned}\frac{dN_{A_1\cdots A_N}(E)}{d\mathbf{R}\ d\mathbf{P}\ dE} &= \prod_{n=1}^{N}\left[\int \frac{d\mathbf{r}_n d\mathbf{p}_n}{h^3}\right]\int dqdp \int d\epsilon\ \rho_{1\cdots N}(\epsilon) \\ &\quad \times\ \delta(E_F - E)\ \delta(\mathbf{P}_F)\ \delta(\mathbf{R}_F)\ \delta(q_F - q)\ \delta(p_F - p) \qquad (12)\\ &= \frac{(2\pi m_0)^{-2}}{\Gamma(\frac{3}{2}N-2)}\prod_{n=1}^{N}\left[(\frac{m_n}{2\pi\hbar^2})^{\frac{3}{2}}\int d\mathbf{r}_n\right]\int dqdp\int d\epsilon\ \rho_{1\cdots N}(\epsilon)\kappa^{\frac{3}{2}N-3}\ \delta(\mathbf{R}_{\mathcal{P}})\ \delta(q_{\mathcal{P}} - q)\ .\end{aligned}$$

In obtaining the second relation, we have carried out the constrained integrations over the momenta $\{\mathbf{p}_n\}$ by use of the formula (D-17).

For given fragment positions $\{\mathbf{r}_n\}$ satisfying the specified constraints, the amount of energy available for statistical sharing between the degrees of freedom of the system is given by

$$E^\star = E - E^0_{1\cdots N} - V(\mathbf{r}_1, ..., \mathbf{r}_N) - k = \kappa + \epsilon\ . \qquad (13)$$

This energy is divided between the random kinetic energy κ of the $3N-4$ remaining translational degrees of freedom of the N fragments and their total internal excitation energy $\epsilon = \sum_n \epsilon_n$. [It is important to note that κ is the energy of the *statistical* motion of the fragments, *i.e.* their motion in addition to the minimal collective motion required for satisfying the specified constraints on the overall momentum $\mathbf{P}$ and the outwards flow p.] For a specified value of the collective outwards kinetic energy $k = p^2/2m_0$, the maximum attainable internal excitation is $\epsilon_k = E^\star$, corresponding to $\kappa = 0$. This (unlikely) situation is achieved when all the fragments move in the radial direction, each with a momentum proportional to its distance from the origin, $\mathbf{p}_n = (m_n p/m_0 q)\mathbf{r}_n$. Moreover, we have $\epsilon_k = \epsilon_{1\cdots N} - k$, where $\epsilon_{1\cdots N} = E - E^0_{1\cdots N} - V$ is the largest possible internal excitation energy, as obtained when the collective kinetic energy k vanishes. This quantity is also the largest value k can have (occurring when $\epsilon_k = 0$), for the particular positions considered.

The above formula (12) "counts" the total number of states (within the given tolerance dE on the total energy) by going through all possible fragmentations F

consistent with the constraints on $\mathbf{R}_F$, $\mathbf{P}_F$, q_F, and p_F, and for each such fragmentation integrating over all values of q and p. The integration over the outwards flow p can be done by elementary means, using the formula

$$\int dp\ \kappa^{\frac{3}{2}N-3} = \sqrt{2\pi m_0}\ \frac{\Gamma(\frac{3}{2}N-2)}{\Gamma(\frac{3}{2}N-\frac{3}{2})}\ (\epsilon_{1\ldots N}-\epsilon)^{\frac{3}{2}N-\frac{5}{2}}\ , \tag{14}$$

which follows from the expression for the volume of a hypersphere. [Of course, for the single purpose of calculating the density of states, there is no need to introduce the variable p in the first place; our reason for doing it here is to pave the way for the calculation of more complicated quantities, such as the transition current to be considered next.]

The disassembly coordinate q controls the overall spatial extension of the multifragment system, while the constrained fragment positions represent orthogonal macroscopic degrees of freedom analogous to the additional deformation parameters employed in refined descriptions of ordinary fission. For purposes of numerical calculations, it is convenient to rewrite the integral over the constrained positions as an average. The corresponding normalization factor is given by the surface area $\Omega'(q)$ of a unit hypersphere,

$$\prod_{n=1}^{N}\left[\int d\mathbf{r}_n\right]\delta(\mathbf{R}_F)\ \delta(q_F-q) = \frac{\sqrt{4\pi}}{\Gamma(\frac{3}{2}N-\frac{3}{2})}\ \left(\frac{m_0}{m_1}\cdots\frac{m_0}{m_N}\right)^{\frac{3}{2}}(\pi q^2)^{\frac{3}{2}N-2}\ , \tag{15}$$

cf. the formula (D-19) derived in Section D.2. It is then readily found that the density of states can be written in the form

$$\begin{aligned} & h^3\ \frac{dN_{A_1\ldots A_N}(E)}{d\mathbf{R}\ d\mathbf{P}\ dE} \\ = & \ \langle\ \frac{2}{\Gamma(\frac{3}{2}N-\frac{3}{2})^2}\int\frac{dq}{q}\ (\frac{m_0q^2}{2\hbar^2})^{\frac{3}{2}N-\frac{3}{2}}\int_0^{\epsilon_{1\ldots N}} d\epsilon\ \rho_{1\ldots N}(\epsilon)(\epsilon_{1\ldots N}-\epsilon)^{\frac{3}{2}N-\frac{5}{2}}\ \rangle' \\ \approx & \ \langle\ \frac{2}{\Gamma(\frac{3}{2}N-\frac{3}{2})}\int\frac{dq}{q}\ (\frac{m_0q^2\bar{\tau}}{2\hbar^2})^{\frac{3}{2}N-\frac{3}{2}}\ \rho_{1\ldots N}(\epsilon_{1\ldots N})\ \rangle'\ . \end{aligned} \tag{16}$$

Here the symbol $\langle\cdot\rangle'$ indicates the average over the constrained fragment positions, and the integral over q extends from the local minimum value $q^{\min}_{1\ldots N}$ (see Appendix A) to the local transition value $q_{1\ldots N}$ (see next Section).

The second line in (16) has been obtained by using the approximate formula (B-7) derived in Section B.1. According to (B-4), the corresponding most probable internal temperature $\bar{\tau}$ is then given by

$$\bar{\tau} = \tau_{1\ldots N}\left\{\left(1+[(\frac{3}{2}N-\frac{5}{2})\frac{\tau_{1\ldots N}}{2\epsilon_{1\ldots N}}]^2\right)^{\frac{1}{2}}-(\frac{3}{2}N-\frac{5}{2})\frac{\tau_{1\ldots N}}{2\epsilon_{1\ldots N}}\right\}\ , \tag{17}$$

The local maximum temperature $\tau_{1\ldots N}$ is related to the local maximum internal excitation by $\epsilon_{1\ldots N} = a_{1\ldots N}\tau^2_{1\ldots N}$. It should also be noted that the most probable

internal excitation energy is given by $\bar{\epsilon} = \epsilon_{1\ldots N} - (\frac{3}{2}N - \frac{5}{2})\bar{\tau}$, as would be expected, since the combined constraints on energy and momentum effectively remove five translational degrees of freedom, each carrying an average kinetic energy of $\frac{1}{2}\bar{\tau}_{1\ldots N}$. The stationary-phase approximation employed is quite adequate for our present purposes. [As noted in Section B.1, an exact analytical formula can be obtained in terms of modified Bessel and Struve functions, see eq. (B-3).]

3.3 Transition current

In order to formulate our transition-state approximation to the disassembly problem, we consider the outwards probability current, *i.e.* the number of elementary multifragment states that pass by a given value of q per unit time. This quantity is given by

$$\begin{aligned} \nu_{A_1\cdots A_N}(E) &= h^3 \frac{(2\pi m_0)^{-2}}{\Gamma(\frac{3}{2}N-2)} \prod_{n=1}^{N} \left[(\frac{m_n}{2\pi\hbar^2})^{\frac{3}{2}} \int d\mathbf{r}_n \right] \\ &\quad \times \int \frac{dp}{h} \frac{p}{m_0} \int d\epsilon\, \rho_{1\ldots N}(\epsilon)\, \kappa^{\frac{3}{2}N-3}\, \delta(\mathbf{R}_F)\, \delta(q_F - q)\ . \end{aligned} \tag{18}$$

The flux factor p/m_0 in the p-integration can be thought of as arising from an integration over values of q extending from 0 to p/m_0, the distance covered by q per unit time. After division by h, the p-integral then yields the number of elementary states that pass the specified value of q per unit time. Since $(p/m_0)dp = dk$, where k is the kinetic energy associated with the outwards flow, the integrations over k and ϵ may be interchanged, so the former one can be performed analytically.

As in the expression (16) for the level density, it is advantageous to express the result in terms of an average over the constrained fragment positions. Proceeding as above, we then find

$$\begin{aligned} &\nu_{A_1\cdots A_N}(E) \\ &= \frac{1}{h} \frac{\sqrt{4\pi}}{\Gamma(\frac{3}{2}N-\frac{3}{2})} \frac{1}{\Gamma(\frac{3}{2}N-1)} \left\langle \left(\frac{m_0 q_{1\ldots N}^2}{2\hbar^2} \right)^{\frac{3}{2}N-2} \int_0^{\epsilon_{1\ldots N}} d\epsilon\, \rho_{1\ldots N}(\epsilon)\, [\epsilon_{1\ldots N} - \epsilon]^{\frac{3}{2}N-2} \right\rangle' \\ &\approx \frac{1}{h} \frac{\sqrt{4\pi}}{\Gamma(\frac{3}{2}N-\frac{3}{2})} \left\langle \left(\frac{m_0 q_{1\ldots N}^2 \bar{\tau}}{2\hbar^2} \right)^{\frac{3}{2}N-2} \rho_{1\ldots N}(\epsilon_{1\ldots N})\, \bar{\tau} \right\rangle' . \end{aligned} \tag{19}$$

Again, we have used the approximation derived in Section B.1 to obtain the second relation, with the temperature $\bar{\tau}$ is given by an expression analogous to (17), but with $\frac{3}{2}N - \frac{5}{2}$ replaced by $\frac{3}{2}N - 2$. It should be noted that although the two mean temperatures $\bar{\tau}$ in the density of states (16) and the transition current (19) are different in principle, they are in practice very similar. In fact, both can usually be replaced by the local maximum temperature $\tau_{1\ldots N}$ without much effect on the results.

3.4 Breakup width

For given values of the constrained positions $\{\mathbf{r}_n\}$, the integrand in the flux (18) has a minimum at some value $q_{1\ldots N}$. Illustrated in figure 1, this key feature is easy to understand since the potential energy has a maximum as the system is stretched from a compact configuration towards separated fragments. This barrier top is a generalization of the conditional saddle point for asymmetric binary fission. The minimum in the integrand will be shifted slightly inwards relative to the barrier top because the geometrical factor q^{3N-4} biases the statistical weights toward larger sizes. As in the treatment of binary fission, it is natural identify the value $q = q_{1\ldots N}$ with the local "bottle neck" in the evolution towards breakup. Accordingly, the total rate at which the system makes an irreversible transition towards disassembly is approximated by the above current (18), with the proviso that the local value of q be chosen as that for which the integrand has a minimum, *i.e.* the transition value $q_{1\ldots N}$.

Invoking the usual statistical assumption, the breakup rate of the system (into the specified mass partition) is given by the magnitude of the transition current, $\nu_{A_1\ldots A_N}(E)$, divided by the total compound level density, $\rho(A,E)$, which represents the total number of elementary states in the decaying compound system. [Both of these refer to states with a total energy within an infinitesimal interval dE around the specified value E.] We then obtain the following approximate relation for the partial width for breakup into specified prefragments,

$$\begin{aligned} \Gamma_{A_1\ldots A_N}(E) &= h\,\frac{\nu_{A_1\ldots A_N}(E)}{\rho(A,E)} \\ &\approx \frac{1}{\rho(A,E)}\,\frac{\sqrt{4\pi}}{\Gamma(\frac{3}{2}N-\frac{3}{2})}\,\langle\,(\frac{m_0 q_{1\ldots N}^2\bar{\tau}}{2\hbar^2})^{\frac{3}{2}N-2}\,\rho_{1\ldots N}(\epsilon_{1\ldots N})\,\bar{\tau}\,\rangle'\,. \end{aligned} \tag{20}$$

We remind of the fact that the average should be taken over the *reduced* fragment positions describing configurations constrained to have a fixed center-of-mass position and a specified (but arbitrary) overall *rms* extension.

4 Discussion

The formula (20) has an intuitive interpretation. It expresses the partial disassembly width Γ as the outwards transition current relative to the total number of states, as in the ordinary transition-state method. The transition current is obtained by adding the contributions from all possible reduced positions of the fragments, corresponding to an integration over the generalized orientation (see Appendix C). For each such generalized orientation, the local transition flux is a product of a macroscopic and a microscopic factor. The macroscopic factor $N_{\text{macro}} \sim \sqrt{4\pi}(m_0 q^2\tau/2\hbar^2)^{\frac{3}{2}N-2}/\Gamma(\frac{3}{2}(N-1))$ is the effective number of states associated with the macroscopic degrees of freedom, *i.e.* those associated with the overall motion of the individual prefragments, while the second factor $\nu_{\text{micro}} \sim \rho\tau$ is the outwards probability current for each such macroscopic state.

4.1 The location of the transition surface

It should be noted that the macroscopic phase-space factor increases in relative importance as the fragment multiplicity N grows. Because of this factor, the transition value of the disassembly coordinate q is shifted somewhat inside the value associated with the maximum in the potential energy of the system. This effect can be analyzed as follows.

The outwards current is proportional to $\langle q^{3N-4}\rho(\epsilon)\tau^{\frac{3}{2}N-1}\rangle'$. We have here used $\epsilon(q)$ to denote the maximum attainable internal energy for a given value of q, $\epsilon = E - E^0_{1\ldots N} - V(q)$, and ignored the small difference between $\tau_{1\ldots N}$ and $\bar{\tau}$, so that $\epsilon \sim \tau^2$ and $\partial \ln \rho/\partial\epsilon = 1/\tau$. In the following simple analysis we shall replace the average over the hypersurface of reduced configurations by a suitably chosen characteristic configuration and consider the behavior of the current when the fragment positions are subjected to an overall scale transformation.

The dominant q-dependence of the current comes from the level density ρ, which depends exponentially on $\epsilon(q)$. This quantity, with or without the temperature factor, is a steadily increasing function of ϵ and so has a minimum where ϵ is the least, *i.e.* where $V(q)$ has its largest value. Let the corresponding value of q be denoted $q_{\rm top}$ and expand $V(q)$ around that point, $V(q) \approx V(q_{\rm top}) + \frac{1}{2}(q - q_{\rm top})^2 V_0''$. It is then straightforward to derive the condition for stationarity of the current. Let the corresponding value of q be denoted q_0. Ignoring the relatively small logarithmic variation of the temperature and we readily obtain

$$\frac{\Delta q}{q_{\rm top}} \approx -(\frac{3}{2}N - 2)\,\frac{E_\perp \tau}{E_q^2} \approx -(\frac{3}{2}N - 2)\,\frac{\tau}{8B_{1\ldots N}} \tag{21}$$

for the shift $\Delta q = q_0 - q_{\rm top}$. In the first relation we have introduced the characteristic energy of the random macroscopic fragment motion, $E_\perp = 2\hbar^2/m_0 q_{\rm top}^2$, and the characteristic energy of the barrier, the "dilaton energy" $E_q = \hbar\sqrt{-V''/m_0}$. In the second relation we have estimated the curvature of the barrier as $V'' \approx -16B/q_{\rm top}^2$, where $B_{1\ldots N}$ denotes the barrier height for the particular channel considered, $B = V(q_{\rm top}) + E^0_{1\ldots N} - E_0$.

Since the transition temperature is typically several MeV, while the barrier heights amount to several tens of MeV, at the least, the reduction in the extension of the transition state is expected to be relatively small. This has been verified by numerical calculations. For example, for ternary breakup of ^{120}Sn (at an excitation energy of around 8 MeV per nucleon) into equal masses we have found $q_{123} \approx 8$ fm with $\Delta q \approx -0.2$ fm, and for breakup into six equal masses $q_{1\ldots 6} \approx 10$ fm with $\Delta q \approx -0.4$ fm.

4.2 The choice of disassembly coordinate

While the specific choice (9-10) of disassembly variables is somewhat arbitrary, the final expression (20) for the decay widths is fairly unique, in the same sense as the standard fission formula (2) is independent of the specific choice of fission coordinate.

To illustrate this important feature, assume that we had preferred to use the *rms* radius of the *total* mass distribution by including the *rms* radii $< r^2 >_n \approx \frac{3}{5}R_n^2$ of the individual fragments in the definition of the disassembly coordinate. We would then have defined the disassembly variables $(\tilde{q}, \tilde{p})$ as follows,

$$\tilde{q}^2 = q^2 + \tilde{q}_0^2 \ , \ \tilde{p} = \frac{\tilde{q}}{q} \ p \ , \tag{22}$$

where $\tilde{q}_0^2 = \sum_n < r^2 >_n$. These variables are also conjugate, as is easily verified, $\{\tilde{p}, \tilde{q}\} = (\partial\tilde{p}/\partial p)(\partial\tilde{q}/\partial q) = 1$. The integration over fragment momenta $\{\mathbf{p}_n\}$ in (12) then yields an extra factor of $q/\tilde{q}$, since $\delta(\tilde{p}) = (q/\tilde{q})\delta(p)$. Moreover, the area of the transition surface (15) is modified to $\tilde{\Omega}'_N(\tilde{q}) = (\tilde{q}/q)\Omega'_N(q)$. These two Jacobian factors cancel each other and, consequently, the expression for the transition current (19) is left unchanged, $\tilde{\nu}_{1\ldots N}(E) = \nu_{1\ldots N}(E)$. It should also be noted that the two averages over the reduced fragment positions are identical, since $\tilde{q}$ determines the same hypersurface as q. The resulting expression (20) for the transition width is then also invariant under the change of disassembly variable.

4.3 Correction for misalignment

In spite of the above demonstrated relative uniqueness of the final formula (20), it is not necessarily optimally accurate, because the actual preferred disassembly path may not coincide with the q direction, *i.e.* the path explored by a scale transformation. This problem is analogous to the phenomenon of misaligned saddles in binary fission occurring when the fission coordinate has been prescribed rather than determined by considering the local normal modes. A correction for this problem can be readily incorporated in our developed formulation, by dividing the local transition flux by $\cos(\alpha)$, where α is the local angle of misalignment. However, $\cos(\alpha)$ is a number of the order of unity, so the effect of this refinement of the preexponential factor is relatively minor, considering that the calculated values of Γ vary over many orders of magnitude, due primarily to the rapid increase of the internal level density with excitation. Since the calculation of the local misalignment angle α is relatively tedious, and has been found to be insignificant, we shall ordinarily omit this correction.

With the compact notation introduced in Appendix C, it is easy to describe an algorithm for calculating the local misalignment angle α. First note that α is determined by $\cos(\alpha) = \hat{\mathcal{N}} \circ \hat{\mathcal{R}}$, where $\hat{\mathcal{N}}$ is the local normal to the transition hypersurface. This normal vector is proportional to the hypergradient of the auxiliary function $f(\vec{\mathcal{R}}) = \mathcal{R} - q_0(\hat{\mathcal{R}})$, where q_0 is the value of q for the transition configuration, as obtained by scaling the reduced fragment positions determined by the hyperdirection $\hat{\mathcal{R}}$.

In practice, the normal $\hat{\mathcal{N}}$ can be obtained by performing small changes in the direction, $\hat{\mathcal{R}} \rightarrow \hat{\mathcal{R}}'$, and then determining the corresponding new transition points $\vec{\mathcal{R}}' = \mathcal{R}'\hat{\mathcal{R}}'$, where $\mathcal{R}' = q_0(\hat{\mathcal{R}}')$. The displacement of the transition point,

$\Delta \vec{\mathcal{R}} = \vec{\mathcal{R}}' - \vec{\mathcal{R}}$ then lies in the hyperplane that is tangent to the transition surface, at the point $\vec{\mathcal{R}}$ considered. By making such a directional change for each Cartesian component of each fragment's position vector $\mathbf{r}_n$, the entire tangent surface can be (redundantly) spanned and the local normal can be obtained from $\vec{\mathcal{R}}$ by subtracting its projection onto the tangent surface, *i.e.* the sum of its components along the $3N$ displacements $\Delta \vec{\mathcal{R}}$.

The inclusion of this refinement has been studied in a variety of scenarios. The magnitude of the misalignment correction increases with multiplicity. For example, for ternary transition configurations, we typically have $< \cos\alpha > \approx 0.9$, whereas for quarternary configurations $< \cos\alpha > \approx 0.5$. Ignoring the misalignment thus introduces a systematic bias against higher multiplicities but, as already noted, the effect is is relatively immaterial since the correction occurs at the preexponential level.

4.4 Binary fission

It is instructive to consider the case of binary splits and discuss the resulting expressions in relation to the standard formulation reviewed in section 1.1. When there are only two fragments present, the averaging over the positions $\mathbf{r}_1$ and $\mathbf{r}_2$ is trivial, since the constraints on the center of mass and the size fix the center separation $r_{12} \equiv |\mathbf{r}_1 - \mathbf{r}_2|$ entirely, so the only macroscopic degrees of freedom of the activated complex are those (two) associated with the overall spatial orientation of the binary complex. It may also be noted that the fission coordinate q is given in terms of the center separation r_{12} by $q^2 = (A_1 A_2 / A^2)\, r_{12}^2$.

For $N = 2$, the two degrees of freedom associated with the hyperdirection $\vec{\mathcal{R}}$ (*i.e.* the reduced fragment positions) correspond to the overall spatial orientation of the dinucleus. Since the potential energy is invariant under an overall spatial rotation, the problem is effectively one-dimensional, as in the standard treatment, and the directional average is trivial. The resulting partial width is then given by

$$\begin{aligned} \Gamma_{A_1 A_2}(E) &= \frac{1}{\rho(A,E)} \frac{2m_0 q_{12}^2}{\hbar^2} \int_0^{\epsilon_{12}} d\epsilon\, \rho_{12}(\epsilon)\, (\epsilon_{12} - \epsilon) \\ &\approx \frac{2m_0 q_{12}^2 \bar{\tau}}{\hbar^2} \frac{\rho_{12}(\epsilon_{12})}{\rho_A(\epsilon_0)}\, \bar{\tau}\,, \end{aligned} \tag{23}$$

where the last relation has been obtained by expanding $\ln \rho_{12}(\epsilon)$ around the upper limit $\epsilon_k = E - E_{12}^0 - V - k$. This expression differs from the one employed in the standard treatment[6] (as reviewed in the Introduction) by the factor $2m_0 q_{12}^2 \bar{\tau}/\hbar^2$. It originates from the relative motion of the two prefragments in directions perpendicular to the radial direction (*i.e.* the line connecting the two prefragment centers) and is thus directly related to the orbital angular momentum of the dinucleus.

A simple physical interpretation of this factor is provided by the fact that the average rotational energy associated with the orbital motion of the binary complex is $< \hbar^2 L^2 / 2m_0 q_{12}^2 > = \bar{\tau}$. Consequently, the factor represents the effective number of

angular-momentum states accessible to the orbital motion system, at the specified elongation of the binary complex. Each value of the orbital angular momentum represents a distinct family of states for the activated complex, thus producing the extra factor.

It is the presence of the two macroscopic degrees of freedom associated with the overall rotation of the binary complex that is responsible for the linear factor in the ϵ-integral, one half power of energy for each degree of freedom. This extra factor produces an additional enhancement of the decay rate for high temperatures, whereas it suppresses the fission width at low temperatures.

It is important to realize that the orbital motion of the binary complex is made physically possible by the fact that each of the two prefragments can carry intrinsic angular momenta, so that the orbital angular momentum can be compensated. In the treatment given in Section 3, the conservation of overall angular momentum has been ignored, in order to facilitate the presentation. In Appendix E the conservation of overall angular momentum is incorporated into the formalism, which in fact introduces little additional complication. The resulting expression for the transition width into a binary channel becomes

$$\Gamma_{A_1A_2}(E,\mathbf{J}) \approx \left[\frac{\mathcal{I}_A\tau_0}{\mathcal{I}_{12}\bar{\tau}}\right]^{\frac{3}{2}} \frac{2m_0q_{12}^2\bar{\tau}}{\hbar^2}\,\frac{\rho_{12}(\epsilon'_{12})}{\rho_A(\epsilon'_0)}\,\bar{\tau}\ , \tag{24}$$

where $\epsilon'_0 = \epsilon_0 - J^2/2\mathcal{I}_A$ and $\epsilon'_{12} = \epsilon_{12} - J^2/2\mathcal{I}_{12}$, with $\mathcal{I}_A$ and $\mathcal{I}_{12}$ being the appropriate moments of inertia. For vanishing total angular momentum, $\mathbf{J} = \mathbf{0}$, there is little difference between the two expressions (23) and (24). In particular, the q-dependent factor remains, so its appearance is *not* an artifact of the fact that angular-momentum conservation was ignored in our derivation of (23).

4.5 Statistical multifragmentation

A variety of conceptually similar statistical models have been developed for nuclear multifragmentation.[2,3,4] They all consider the statistical equilibrium of N fragments which are confined within some suitable freeze-out volume Ω and assumed to satisfy certain constraints, such as energy conservation. It is instructive to compare the treatment developed in the present work with such statistical models. In order to facilitate the discussion, we shall specifically compare with the formulation made in ref. [2], since our treatment conforms to the notation introduced there.

In that model, the yield of a given multifragment channel $A_1, ..., A_N$ is taken to be proportional to the microcanonical weight of that particular mass partition. In our present notation, this quantity is given by the expression (7), so we have

$$\Gamma^{\text{stat}}_{A_1\cdots A_N}(E) \sim \frac{dN_{A_1\cdots A_N}(E)}{d\mathbf{R}\ d\mathbf{P}\ dE}\ . \tag{25}$$

This quantity can be compared with the expression (18) for the disassembly current to which our transition width is proportional. By proceeding as in Section 3, the

integrations over the fragment momenta $\{\mathbf{p}_n\}$ can be carried out analytically, and those over the internal excitation energies can be combined into a single integration over the total internal excitation energy ϵ, leading to

$$\Gamma^{\text{stat}}_{A_1\cdots A_N}(E) \sim \frac{(2\pi m_0)^{-\frac{3}{2}}}{\Gamma(\frac{3}{2}N-\frac{3}{2})} \prod_{n=1}^{N} \left[\int d\mathbf{r}_n (\frac{m_n}{2\pi\hbar^2})^{\frac{3}{2}}\right] \int d\epsilon\ \rho_{1\cdots N}(\epsilon)\ E_{\text{kin}}^{\frac{3}{2}N-\frac{5}{2}} \ . \tag{26}$$

Here E_{kin} denotes the total kinetic energy of the fragments. In our transition-state treatment this energy is shared between the collective outwards motion and the random motion of the prefragments. Since the statistical multifragmentation model does not contain collective variables, such a division of E_{kin} is not relevant.

In (26) the integrations over the fragment positions $\{\mathbf{r}_n\}$ are constrained by demands that the overall center of mass position remain at the origin and each of the fragment positions remain within the specified volume Ω. [The center-of-mass constraint has usually been ignored, but we shall include it here for ease of comparison.] The determination of the freeze-out volume is external to the model. For the purposes of our present comparison, we shall assume that the freeze-out volume corresponds to the volume enclosed by the transition surface determined by the developed transition-state treatment. The statistical multifragmentation width can then be written on the form

$$\Gamma^{\text{stat}}_{A_1\cdots A_N}(E) \sim \frac{(2\pi m_0)^{-\frac{3}{2}}}{\Gamma(\frac{3}{2}N-\frac{3}{2})} \prod_{n=1}^{N} \left[\frac{m_n}{2\pi\hbar^2}\right]^{\frac{3}{2}} \langle\ \Omega_N(q_{1\cdots N}) \int d\epsilon\ \rho_{1\cdots N}(\epsilon)\ E_{\text{kin}}^{\frac{3}{2}N-\frac{5}{2}}\ \rangle'_{q<q_{1\cdots N}} \ . \tag{27}$$

Here the average includes all fragment positions $\{\mathbf{r}_n\}$ for which the associated disassembly coordinate q is less than the local transition value $q_{1\cdots N}$. The associated normalization factor is given by the hypervolume enclosed by the transition surface,

$$\Omega_N(q_0) \equiv \int_0^{q_{1\cdots N}} dq\ \Omega'_N(q_{1\cdots N}) \ = \ \frac{(\pi q^2_{1\cdots N})^{\frac{3}{2}N-\frac{3}{2}}}{\Gamma(\frac{3}{2}N-\frac{1}{2})} (\frac{m_0}{m_1}\cdots\frac{m_0}{m_N})^{\frac{3}{2}} \ , \tag{28}$$

using the result (15) for the hypersurface area. Insertion of this formula into (26) then yields the result

$$\begin{aligned}
&\Gamma^{\text{stat}}_{A_1\cdots A_N}(E) \sim \\
&\frac{1}{\Gamma(\frac{3}{2}N-\frac{1}{2})}\ \frac{1}{\Gamma(\frac{3}{2}N-\frac{3}{2})} \langle\ (\frac{m_0 q^2_{1\cdots N}}{2\hbar^2})^{\frac{3}{2}N-\frac{3}{2}} \int d\epsilon\ \rho_{1\cdots N}(\epsilon)\ (\epsilon_0-\epsilon)^{\frac{3}{2}N-\frac{5}{2}}\ \rangle_{q<q_{1\cdots N}} \\
&\approx \frac{1}{\Gamma(\frac{3}{2}N-\frac{1}{2})} \langle\ (\frac{m_0 q^2_{1\cdots N}\bar{\tau}}{2\hbar^2})^{\frac{3}{2}N-\frac{3}{2}}\ \rho_{1\cdots N}(\epsilon_0)\ \rangle_{q<q_{1\cdots N}} \ .
\end{aligned} \tag{29}$$

The above form of the statistical multifragmentation model is very convenient for comparisons with our present treatment. While the general form of (29) for Γ^{stat} is rather similar to our result (18) for the transition current $\nu_{1\cdots N}(E)$, several notable differences exist, as discussed below.

One important difference is that the position average in the statistical model includes the entire volume inside the transition surface, $q < q_{1\cdots N}$, rather than merely

those configurations that have $q = q_{1\ldots N}$. The more compact the configuration, the better the system is generally bound, so that the statistical weight is correspondingly larger. This feature will tend to favor configurations with small values of q, although the geometrical factor proportional to q^{3N-4} will produce a counteracting bias towards large values of q.

The two treatments also differ by the fact that the statistical multifragmentation model has one power of q more, as well as an extra factor of $(m_0 q_{1\ldots N}^2 \tau / 2\pi\hbar^2)^{\frac{1}{2}}$. The former difference arises from the fact that the phase space associated with the fragment positions has one dimension more, since all values $q < q_{1\ldots N}$ are included. The extra factor arises for the same reason, since there is then one less constraint on the macroscopic motion of the fragments and an additional power of the associated phase space is present.

Finally, whereas the standard statistical multifragmentation models produce essentially final fragments (possibly subject to post-breakup evaporation), the present treatment yields interacting prefragments whose post-transition evolution can lead to significant changes in fragment multiplicity, mass, and energy. In fact, our transition configurations should be regarded as initial conditions for a suitable dynamical calculation of the further disassembly process. Such a refined treatment of the post-transition evolution is more difficult to formulate in the standard statistical models which do not take explicit account of the appropriate potential barriers.

4.6 Evolution of prefragment multiplicity with energy

We close this general discussion of the transition-state formulation by considering the evolution of the breakup width with energy. Generally, the partial width $\Gamma_{A_1\ldots A_N}(E)$ increases steadily as a function of the excitation energy in the source, $\epsilon_0 = E - E_0$. Moreover, because the transition current $\nu_{A_1\ldots A_N}(E)$ depends on the *rms* extension q via a power proportional to the fragment multiplicity, the increase with energy is steeper for higher multiplicities. Consequently, at some energy multiple breakup will start to dominate over binary splits. This feature is illustrated in figure 2, which displays the total width $\Gamma_A^N(E)$ for breakup of ^{120}Sn into N prefragments, each with a mass number larger than ten. As defined in (20), this quantity is obtained by adding the partial widths $\Gamma_{A_1\ldots A_N}(E)$ associated with all possible mass partitions of the given source (with the restriction $A_n > 10$).

It is seen that the total width for ternary breakup overtakes the total binary width at a little above 2 MeV per nucleon, only to be overtaken by the total quarternary width about one MeV later. This pattern continues for the higher multiplicities, but the succession of dominance occurs increasingly rapidly as a function of the energy, so that around four MeV per nucleon the breakup is dominated by high values of N. It is important to be aware that that the displayed quantity $\Gamma_A^N(E)$ is the width for the breakup into *pre*fragments, rather than final fragments. Indeed, these prefragments are to be employed as *initial* conditions in a subsequent dynamical calculation, for the purpose of determining the characteristics of the ac-

tual final channel. For all values of N larger than two, significant recoalescence is expected in the course of the post-breakup disassembly, because the transition configuration will almost certainly contain fragment pairs that are situated inside their respective binary potential barrier and these are then likely to fuse with each other as the system evolves.

The most important qualitative effect of the post-transition dynamics is that the final fragment multiplicity will be lower than the prefragment multiplicity. Therefore, the results displayed in figure 2 should not be taken to indicate that a transition from binary splits to multifragmentation will occur already at an excitation of 2-3 MeV per nucleon. Rather, it should be expected that incorporation of post-transition coalescence will move the cures upwards in energy by a few MeV.

It appears difficult to devise a simple method for predicting the outcome of the post-transition dynamics. We feel that a relatively reliable method (yet a reasonably simple and cost-effective one) consists in solving the coupled equations of motion for the N prefragments by adapting treatments developed in studies of damped nuclear reactions. We shall present this part of the treatment in a subsequent paper.[7]

5 Concluding remarks

We have formulated a transition-state approximation for the disassembly of an excited compound nucleus into multi-fragment final channels. By describing the transition configuration as a collection of interacting prefragments, the partial decay width is expressed as the ratio between the outwards flow rate and the level density of the compound nucleus. At low excitation, channels with only two fragments dominate and the formula for the decay width reduces to a form rather similar to the standard Bohr-Wheeler expression, but with an extra factor arising from the orbital motion of the binary complex. The dominant multiplicity increases with excitation and at high excitation the treatment acquires considerable formal similarity with standard statistical multifragmentation models, although certain notable differences are present. An important advantage of the treatment is that it automatically provides the constraint on the fragment positions so that a finite result is obtained; in this regard it is a significant advance relative to current statistical models in which the freeze-out volume must be prescribed separately.

This novel transition-state treatment of multifragmentation provides a well-defined means for calculating the partial widths for transition of the system into a number of interacting prefragments with specified masses and total energy. In order to obtain the actual final channel for a particular disassembly process, it is necessary to follow the further propagation of the system from the transition point towards asymptotia, since some prefragment pairs may find themselves inside the barrier of their respective two-body interaction potential and hence may recombine. We plan to address this important question in a subsequent paper.[7]

A major motivation for undertaking the present work has been the need for a model in which the evolution of the disassembly process from low to high excitation

can be addressed. Having attractive limits, the developed model provides such a framework and its utility has been illustrated by our studies of the dependence of the (pre)fragment multiplicity on excitation energy. Though depending on Monte-Carlo sampling, the application of the model is not more computer-demanding than current statistical multifragmentation models, and a variety of instructive applications of the model are foreseen, at this point primarily for the purpose of gaining theoretical insight. The application of the method to observable quantities must await the incorporation of the post-transition of the prefragment complex into well-separated fragments.

We wish to acknowledge considerable help by W.J. Swiatecki regarding the development of the potential-energy function. We also wish to thank him, Thomas Døssing, George Fai, Sean Gavin, Matthias Grabiak, and Andrew Jackson for helpful and stimulating discussions. This work was supported by the Director, Office of Energy Research, Office of High Energy and Nuclear Physics, Division of High Energy Physics, of the U.S. Department of Energy under Contract No. DE-AC03-76SF00098.

A Potential energy

The potential energy of a transition configuration forms a practically important ingredient in our formulation. We describe below how a relatively simple approximate scheme can be devised for the calculation of this quantity. The specific form adopted here is expected to be replaced by more accurate results as they become available. It is important to note, though, that our entire transition-state formulation does not rely on any specifics of the interaction potential, except that it be independent of the fragment momenta, and we only describe the particular form adopted for the sake of completeness.

To estimate the potential energy of the system at the transition point, we assume that the multifragment configuration at this point consists of distinct prefragments with mass numbers $A_1, ..., A_N$, as argued for above. For simplicity, the isospin degrees of freedom are ignored and the charge numbers of the prefragments are chosen so as best to preserve the charge-to-mass ratio characteristic of the system. Though somewhat tedious, it would be straightforward to include the charge numbers as degrees of freedom; that should preferably be done before quantitative predictions or comparisons are made.

Since the transition configurations typically consist of well-developed prefragments, we shall assume that the total potential energy V associated with a given positioning $\{\mathbf{r}_n\}$ of the fragments can be expressed as a sum of pairwise interaction energies,

$$V(\mathbf{r}_1, ..., \mathbf{r}_n) = \sum_{n<n'} V_{nn'}(r_{nn'}) \ , \qquad \text{(A-1)}$$

where $r_{nn'} \equiv |\mathbf{r}_n - \mathbf{r}_{n'}|$. The individual terms $V_{nn'}$ will be carefully designed so as

to yield a reasonable global description of the potential energy of a binary system.

In order to achieve this, we consider an arbitrary binary channel characterized by the mass numbers $\{A_1 A_2\}$. Let the two (pre)fragments have the center separation r_{12} and let the corresponding potential energy be $E_{12}(r_{12})$. The "interaction energy" between the two fragments can then be defined as

$$V_{12}(r_{12}) \equiv E_{12}(r_{12}) - E_1^0 - E_2^0 \ , \tag{A-2}$$

where E_1^0 and E_2^0 are the ground-state energies of the two individual fragments. For these we use the Lysekil mass formula [8],

$$E_A^0 = (-a_1 A + a_2 A^{\frac{2}{3}})(1 - I^2) + c_3 \frac{Z^2}{A^{\frac{1}{3}}} \ , \tag{A-3}$$

with a_1=15.4941, a_2=17.9439, κ=1.7826, c_3=0.70535, and $I = (N - Z)/A$.

As a first step towards constructing a suitable potential function, let us concentrate on the (conditional) saddle-point energy, $E_{12}^{\rm top}$. This quantity is the maximum potential energy of the system as it develops along the fission path, starting from the spherical compound shape and ending with two separated spherical fragments having the specified mass numbers A_1 and A_2. To estimate $E_{12}^{\rm top}$, we use an approximate expression for the saddle-point energy recently developed by Swiatecki.[9]

Swiatecki introduces a fissility parameter x_0 that is equal to 6/5 times the standard value,

$$x_0 = \frac{6}{5} \frac{e^2 Z^2}{16\pi\gamma R_0^3} \ , \tag{A-4}$$

and a corresponding effective fissility

$$x_{\rm eff} = \frac{6}{5} \frac{e^2 Z_1 Z_2}{4\pi\gamma \bar{R}(R_1 + R_2)^2} \tag{A-5}$$

as the generalization to mass-asymmetric shapes, where $\bar{R} = R_1 R_2/(R_1 + R_2)$. Parametrizing the nuclear configuration at the saddle point as two spheres connected by a conical neck, Swiatecki then obtains the following expression for the energy of the conditional saddle point and the corresponding center separation,

$$\begin{aligned} E_{12}^{\rm top} &= 4\pi^2\gamma \, [u^2 + w^2 - 1 + \frac{12}{5} x_0 (u^5 + w^5 - 1 + \frac{5}{3} \frac{u^3 w^3}{u + w}) \\ &\quad + 2(\frac{uw}{u+w})^2 (-x_{\rm eff}^2 + x_{\rm eff}^3 - \sigma_1 x_{\rm eff}(1 - x_{\rm eff})^2)] \\ r_{12}^{\rm top} &= (R_1 + R_2) \left[(1 - \Delta^2)(2x_{\rm eff}^2 - 3x_{\rm eff}^3 + \sigma_1(1 - 4x_{\rm eff} + 3x_{\rm eff}^2)) + 1 \right]^{\frac{1}{2}} \ . \end{aligned} \tag{A-6}$$

Here $u = R_1/R_0$ and $w = R_2/R_0$, where $R_n = r_0 A_n^{1/3}$ are the equivalent sharp radii of the fragments and $R_0 = r_0 A^{1/3}$ is the radius of the compound nucleus (the radius parameter has the value $r_0 = 1.224992$ fm). The specific surface tension is given by $\gamma = a_2/4\pi r_0^2$. Furthermore, the quantity $\Delta = (R_1 - R_2)/(R_1 + R_2)$

provides a convenient measure of the mass asymmetry and it is easily seen that $x_{\text{eff}} \sim (1-\Delta^2)^2/(1+3\Delta^2)$.

Relative to Swiatecki's original formulation[10], the parts containing the variable $\sigma_1 = s_1/2\bar{R}$ in (A-6) have been added to mimic the effect of the finite range of the nuclear interaction on the barrier energies, as done in ref. [11]. The "proximity shift" s_1 represents the inwards effective shift in the fragment interaction potential caused by the attractive nuclear forces between the two fragments and is taken to have the value $s_1 = 2$ fm. The ensuing formula for E_{12}^{top} leads to a reasonable global behavior of the fission barrier, both for symmetric and asymmetric fission, as illustrated in figure 3. The results are far from perfect, though, and considerable quantitative improvement is needed regarding the calculation of the barrier energies.

With this prescription for E_{12}^{top} and r_{12}^{top}, it is fairly straightforward to construct a useful interaction potential function $V_{12}(r_{12})$. For shapes more compact than the saddle configuration, *i.e.* for $r_{12}^{\min} \leq r_{12} \leq r_{12}^{\text{top}}$, we interpolate between the saddle and the ground state, which has the energy E_0 and the center separation $r_{12}^{\min} = |R_1 - R_2|$. Using a cubic spline in r_{12}, we ensure that the resulting potential function has a minimum at $r_{12} = r_{12}^{\min}$ and a maximum at r_{12}^{top}. It should be pointed out that we restrict our considerations to such multifragment configurations for which all prefragment pairs ij have a center separation r_{ij} in excess of the corresponding minimum value $r_{ij}^{\min}$.

Beyond the saddle, we seek to match with the asymptotic Coulomb potential $V_{12}(r_{12}) = e^2 Z_1 Z_2 / r_{12}$ at a suitable separation $r_{12}^{\max} > r_{12}^{\text{top}} + R_1 + R_2$. Again a cubic spline is used, so that $V_{12}(r_{12})$ has a maximum at the saddle and joins the asymptotic form smoothly at $r_{12} = r_{12}^{\max}$.

The prescription described above grows rather inaccurate when small fragments are considered, as might be expected since macroscopic formulas are employed. Therefore, we shall limit our calculational applications to configurations containing only fragments with $A > 10$. For such configurations, any refinement in $V_{12}(r_{12})$ is expected to have rather little effect on the results: the prescription is by design accurate for binary channels, while for multifragment configurations the associated averaging over the spatial positioning of the fragments will tend to sample a rather broad range of separation values, thus reducing the sensitivity to refinements. [Any refinements must be fairly local, since our potential function is expected to have a good global behavior, having been matched at small, intermediate, and large values of the separation variable.]

Figure 4 shows an example of how V_{12} varies with the fragment separation r_{12} for several mass partitions of ^{120}Sn. The three different sections of the curves correspond to the three regions described above: inside the saddle ($r_{12}^{\min} \leq r_{12} \leq r_{12}^{\text{top}}$), outside the saddle ($r_{12}^{\text{top}} \leq r_{12} \leq r_{12}^{\max}$), and in the asymptotic (Coulomb) region ($r_{12}^{\max} \leq r_{12}$). Also shown are the saddle points (solid circles) and the points corresponding to tangent spheres (solid squares). In this particular case, the saddle-point configuration is represented by non-intersecting spheres for large mass asymmetries, whereas the two spheres overlap for more symmetric splits.

With the binary interaction potential determined as described above, the interaction energy V in (A-1) can then be calculated, provided that all the pairwise fragment separations are larger than their respective minimum value, *i.e.* $r_{nn'} \geq r_{nn'}^{\min}$. Only multifragment configurations satisfying this condition are considered.

Figure 5 shows some transition configurations for breakup of the nucleus ^{120}Sn into three or four fragments with specified masses. It is seen that the configurations have a distinct multifragment character, with the individual prefragments rather well developed, *i.e.* the pairwise overlaps are relatively small. For larger multiplicities the transition-state configurations tend be generally better developed, although the relative frequency of configurations with some pair having considerable overlap also increases, suggesting that a recoalescence is likely to occur subsequent to the transition. By examining many such randomly chosen saddle-point configurations of various multiplicities, we have concluded that the prefragments are usually fairly well developed. This feature lends support to our parametrization of the transition state in terms of the degrees of freedom associated with a number of distinct fragments. [This property does not hold for binary splits of heavy nuclei, but this poses no problem, since the potential-energy function $V_{12}(r_{12})$ has been carefully designed to exhibit a reasonable global behavior for $N = 2$.] It should be kept in mind, though, that our assumption that the potential energy can be expressed in terms of pairwise interactions breaks down for compact configurations, so caution should be exercised if the energy of such configurations is needed.

B Internal level density

As in the standard fission treatment, we need to know the density of internal excitations in the system. For a single nucleus, it often suffices to employ a simple Fermi-gas form,

$$\rho_A(\epsilon) \;=\; c\, A^{-p}\, e^{2\sqrt{a_A \epsilon}}\,. \qquad \text{(B-1)}$$

With $p = \frac{1}{2}$, $c = 0.002/\text{MeV}$, and $a_A = (A-1)/8$ MeV a reasonable correspondence is obtained with the mass dependence of the nuclear level density at an excitation energy of 7 MeV, as obtained by absorption of thermal neutrons. Of course, 7 MeV is a very small excitation in the present context and the above formula should not be trusted quantitatively at high excitation. However, the above formula suffices for the formulation of our treatment, as well as for qualitative studies of global features.

It should be noted that we are using $A-1$ rather than A in the level density parameter a_A in order to take approximate account of the conservation of overall CM position and momentum which removes three translational degrees of freedom from the system. Though rather unimportant for a single large nucleus, this refinement becomes increasingly significant as the fragment multiplicity increases.

The above simple formula ignores the possibility of a pre-exponential energy dependence and also neglects any dependence of the parameters on nuclear size,

shape, and temperature. These refinements are all interesting, and often quantitatively important. However, their precise forms are not yet well established. The situation is even less clear for the internal level density $\rho_{1\ldots N}(\epsilon)$ of the transition configurations needed in the present multifragmentation theory. These configurations are described in terms of N prefragments and can be regarded as somewhat intermediate between a very distorted single nucleus and a collection of distinct fragments.

Notwithstanding the many theoretical uncertainties associated with calculating the internal level density for a multifragment transition configuration, we employ the simple Fermi-gas formula (B-1) for the internal level density of the individual prefragments as well. The combined internal level density $\rho_{1\ldots N}(\epsilon)$, which is given as the corresponding multiple convolution, can then be expressed in a simple form by generalizing the stationary-phase approximation used in ref. [13].

B.1 Integration over internal excitation

In our treatment we need to evaluate integrals of the form

$$\mathcal{I}_n(\epsilon_0) = \int_0^{\epsilon_0} d\epsilon\ \rho(\epsilon)\ (\epsilon_0 - \epsilon)^n\ , \tag{B-2}$$

where $n \geq 0$ in our present applications. For the standard form $\rho \sim \exp(2\sqrt{a\epsilon})$, as we assume throughout, the above integral can be expressed on analytical form,

$$\mathcal{I}_n = \epsilon_0^{n+1}\left[\frac{1}{n+1} + \sqrt{\pi}\ \Gamma(n+1)\ (a\epsilon_0)^{-n-\frac{1}{2}}\{I_{n+\frac{3}{2}}(2\sqrt{a\epsilon_0}) + \mathbf{L}_{n+\frac{3}{2}}(2\sqrt{a\epsilon_0})\}\right]\ , \tag{B-3}$$

where I_ν and $\mathbf{L}_\nu$ are the modified Bessel and Struve functions, respectively.[14] The standard analytical representations of these special functions can then be employed for an exact evaluation of $\mathcal{I}_n(\epsilon_0)$.

Since such a procedure would be fairly tedious, it is desirable to employ a simple approximation. This can be achieved by evaluating the integral in the stationary-phase approximation. Towards this end, the logarithm of the integrand can be expanded to second order in ϵ. The demand that it be stationary yields the relation $\epsilon_0 - \epsilon_n = n\tau_n$ for the most probable intrinsic excitation ϵ_n, around which the expansion should be made. The temperature τ_n is the inverse of $\partial \ln \rho/\partial\epsilon$ and for a level density of standard Fermi-gas form ($\ln\rho \sim 2\sqrt{a\epsilon}$) we have $\epsilon_n = a\tau_n^2$. The temperature is then readily found to be

$$\tau_n = \tau_0\left([1 + (\frac{n\tau_0}{2\epsilon_0})^2]^{\frac{1}{2}} - \frac{n\tau_0}{2\epsilon_0}\right)\ , \tag{B-4}$$

where τ_0 is the maximum temperature, $\epsilon_0 = a\tau_0^2$. The second derivative is also easy to calculate,

$$\frac{1}{\sigma_n^2} = \frac{\partial^2}{\partial\epsilon^2}\ln[\rho(\epsilon)(\epsilon_0 - \epsilon)^n] = \frac{1}{2\epsilon_n\tau_n} + \frac{1}{n\tau_n^2} = \frac{2\epsilon_n + n\tau_n}{2n\epsilon_n}\ \frac{1}{\tau_n^2}\ , \tag{B-5}$$

and the integral of the resulting Gaussian function then yields

$$\mathcal{I}_n(\epsilon_0) = \sqrt{2\pi\sigma_n^2}\ \rho(\epsilon_n)\ (\epsilon_0 - \epsilon_n)^n = \left[2\pi n \frac{2\epsilon_n}{2\epsilon_n + n\tau_n}\right]^{\frac{1}{2}}\ \tau_n\ \rho(\epsilon_n)\ [n\tau_n]^n \quad (B\text{-}6)$$

$$\approx \left[\frac{2\epsilon_n}{2\epsilon_n + n\tau_n}\right]^{\frac{1}{2}}\ \tau_n\ \Gamma(n+1)\ (\tau_n e)^n\ \rho(\epsilon_n) \quad (B\text{-}7)$$

$$\approx \Gamma(n+1)\ \rho(\epsilon_0)\ \tau_n^{n+1}\ . \quad (B\text{-}8)$$

The second relation (B-7) has been obtained by use of Stirling's formula.[14] This approximation is quite accurate for large values of n and overestimates the result (B-6) by only 8% for $n = 1$. The last relation (B-8) follows by assuming that $n\tau_n \ll 2\epsilon_n$ (so that the square root gives unity) and recognizing that $e^n\rho(\epsilon_n) \approx \rho(\epsilon_0)$. This latter relation can also be obtained more directly by expanding $\rho(\epsilon)$ in (2) to first order around ϵ_n.

It should be noted that the above derivation of (B-6) does not apply for $n = 0$, since there is then no stationary point. Instead, the (rapidly increasing) integrand can be expanded to first order around the upper limit ϵ_0, leading to $\mathcal{I}_0(\epsilon_0) = \tau_0\rho(\epsilon_0)$. It is a special advantage of the approximate formulas (B-7) and (B-8) that they can be evaluated also for $n = 0$ (whereas the exact formula (B-6) is ill-defined for $n = 0$) and in fact yield precisely the desired result, $\mathcal{I}_0(\epsilon_0) = \tau_0\rho(\epsilon_0)$.

It should be pointed out, though, that the above approximate formulas may yield somewhat inaccurate results. If high accuracy is required, it might be preferable to use the analytical expression (B-3) or resort to a direct numerical integration of (B-2). In our present applications, we prefer to use the approximate formula (B-8) because it is simple and transparent, and yet quite accurate. It has been verified by direct calculation that it provides a quite satisfactory accuracy in the mass and energy ranges of primary interest in the present context. For example, for the (rather extreme) case of binary disassembly of a system with $A = 20$ and $\epsilon_0/A = 2$ MeV, the formula (B-8) is at most 10% too low, and it rapidly improves as either A or ϵ_0 is increased; moreover, Stirling's approximation improves dramatically as n is increased. When judging the utility of the approximation, it should be remembered that the integrals $\mathcal{I}_n(\epsilon_0)$ are strongly varying functions, spanning many orders of magnitude, so inaccuracies at the percentage level are fairly immaterial; in particular, they will have little effect on calculated energy thresholds, such as the energy for which the width for ternary disassembly equals that for binary breakup.

C Condensed multifragment notation

For discussion of multifragmentation problems, it is convenient to introduce a compact notation. First we note that the positions $\{\mathbf{r}_n\}$ of the N fragments can be represented by a single point in a $3N$-dimensional hyperspace,

$$\vec{\mathcal{Q}} = \left(\sqrt{\frac{m_1}{m_0}}\ \mathbf{r}_1, \ldots, \sqrt{\frac{m_N}{m_0}}\ \mathbf{r}_N\right)\ , \quad (C\text{-}1)$$

where $m_0 = \sum_n m_n$. The (square of) the norm of this hypervector is $\mathcal{Q}^2 = \vec{\mathcal{Q}} \circ \overleftarrow{\mathcal{Q}} = (1/m_0)\sum_n m_n \mathbf{r}_n^2$, and the corresponding normalized directional vector is $\hat{\mathcal{Q}} = \vec{\mathcal{Q}}/\mathcal{Q}$. It is usually preferable to refer the fragments to the location of the center of mass, $\mathbf{R} = (1/m_0)\sum m_n \mathbf{r}_n$. Therefore it is convenient to introduce the following *reduced* position vector

$$\vec{q} = q\hat{q} = (\sqrt{\frac{m_1}{m_0}}\,(\mathbf{r}_1 - \mathbf{R}), ..., \sqrt{\frac{m_N}{m_0}}\,(\mathbf{r}_N - \mathbf{R}))\ , \qquad (C\text{-}2)$$

which is confined to the $(3N\text{-}3)$-dimensional hyperplane of configurations with vanishing CM position. Its modulus q is identical to the disassembly coordinate introduced in (9), as is readily verified by calculating the square, $q^2 = \vec{q} \circ \overleftarrow{q} = \mathcal{Q}^2 - R^2$.

A similar notation can be introduced for the fragment momenta $\{\mathbf{p}_n\}$. Thus we define the hypermomentum of a particular fragmentation as

$$\vec{\mathcal{P}} = (\sqrt{\frac{m_0}{m_1}}\,\mathbf{p}_1, ..., \sqrt{\frac{m_0}{m_N}}\,\mathbf{p}_N)\ , \qquad (C\text{-}3)$$

and note that $\mathcal{P}^2 = \vec{\mathcal{P}} \circ \overleftarrow{\mathcal{P}} = 2m_0 T$, where $T = \sum_n p_n^2/2m_n$ is the total kinetic energy of the N fragments.

Again it is convenient to transform to the CM frame, and so we introduce the following reduced hypermomentum,

$$\vec{p} = (\sqrt{\frac{m_0}{m_1}}\,(\mathbf{p}_1 - m_1\mathbf{V}), ..., \sqrt{\frac{m_0}{m_N}}\,(\mathbf{p}_N - m_N\mathbf{V}))\ , \qquad (C\text{-}4)$$

where $\mathbf{V} = \mathbf{P}/m_0$ is the CM velocity. We note that the radial component of the reduced hypermomentum is identical to the radial flow p introduced in (10), as is readily verified by projecting $\vec{p}$ onto $\hat{q}$,

$$\vec{p} \circ \hat{q} = \frac{1}{q}\,\vec{p} \circ \overleftarrow{q} = \frac{1}{q}(\sum_{n=1}^{N} \mathbf{p}_n \cdot \mathbf{r}_n - \mathbf{P} \cdot \mathbf{R})\ . \qquad (C\text{-}5)$$

We note that the density of states for a given mass partition (7) can be expressed in the compact notation as

$$\frac{dN_{A_1 \cdots A_N}(E)}{d\mathbf{R}\ d\mathbf{P}\ dE} = \int \frac{d\mathcal{Q}d\mathcal{P}}{h^{3N}} \int d\epsilon\ \rho_{1\cdots N}(\epsilon)\ \delta(E_F - E)\ \delta(\mathbf{P}_F)\ \delta(\mathbf{R}_F)\ . \qquad (C\text{-}6)$$

We also note that the integral (15) over the reduced fragment positions can be reexpressed as an angular integral in the reduced hyperspace,

$$\prod_{n=1}^{N}\left[\int d\mathbf{r}_n\right]\delta(\mathbf{R}_F)\ \delta(q_F - q) = \prod_{n=1}^{N}\left[\frac{m_0}{m_n}\right]^{\frac{3}{2}} \int d\,\vec{\mathcal{Q}}_F\ \ \delta(\mathbf{R}_F)\ \delta(q_F - q) \qquad (C\text{-}7)$$

$$= \prod_{n=1}^{N}\left[\frac{m_0}{m_n}\right]^{\frac{3}{2}} \int d\,\vec{q}_F\ \ \delta(q_F - q) = \prod_{n=1}^{N}\left[\frac{m_0}{m_n}\right]^{\frac{3}{2}} \int d\hat{q}_F\ q_F^{3N-4}$$

$$= \frac{2}{\Gamma(\frac{3}{2}N - \frac{3}{2})}\ \langle \int \frac{dq}{q}\ (\pi q^2)^{\frac{3}{2}N - \frac{3}{2}}\ \rangle'\ ,$$

where it has been used that $d\vec{q} = q^{3N-4} dq d\hat{q}$ and that

$$\int d\hat{q} = \prod_{n=1}^{N} \left[\frac{m_n}{m_0}\right]^{\frac{3}{2}} \Sigma_{3N-3} , \tag{C-8}$$

with $\Sigma_n = 2\pi^{\frac{3}{2}n}/\Gamma(\frac{3}{2}n)$ denoting the surface area of a unit sphere in n dimensions. In the last relation the average is over the reduced hyperdirection $\hat{q}$, which is the same as averaging over the reduced positions.

D Microcanonical phase space

The treatment developed in the present work requires the evaluation multiple integrals over the fragment positions and momenta subject to certain constraints. We show below how these integrals can be performed analytically by exploiting the following Fourier representation of the δ-function,

$$\delta(E) = \int_{-\infty}^{+\infty} \frac{dt}{h} \exp(\frac{i}{\hbar} Et) . \tag{D-1}$$

D.1 Energy conservation

We first consider the constrained momentum integral arising when overall energy conservation is imposed on a system of free particles,

$$\mathcal{I}_N(E) \equiv \prod_{n=1}^{N} \left[\int d\mathbf{p}_n\right] \delta(\sum_{n=1}^{N} \frac{p_n^2}{2m_n} - E) , \tag{D-2}$$

where E is the specified total kinetic energy of the N particles. This integral can be evaluated in a variety of ways. For our present purposes, we find it most convenient to exploit the above Fourier representation (D-1) and so obtain

$$\begin{aligned} \mathcal{I}_N(E) &= \int \frac{dt}{h} \exp(\frac{i}{\hbar} Et) \prod_{n=1}^{N} \left[\int d\mathbf{p}_n \exp(-\frac{i}{\hbar}\frac{p_n^2}{2m_n} t)\right] \\ &= \int \frac{dt}{h} \exp(\frac{i}{\hbar} Et) \prod_{n=1}^{N} \left[\frac{hm_n}{it}\right]^{\frac{3}{2}} = \frac{2\pi}{\Gamma(\frac{3}{2}N)} (m_1 \cdots m_N)^{\frac{3}{2}} [2\pi E]^{\frac{3}{2}N-1} . \end{aligned} \tag{D-3}$$

To obtain the last relation, we have used the representation of the Γ-function in terms of Hankel's Contour Integral [14]. The result is quite reasonable, since the total number of translational degrees of freedom, $3N$, is reduced by two as a consequence of the demand that the system be on the energy shell specified by E.

D.2 Energy and momentum conservation

When overall momentum conservation is also imposed, the following integral needs to be evaluated,

$$\mathcal{I}_N(\mathbf{P}, E) \equiv \prod_{n=1}^{N} \left[\int d\mathbf{p}_n\right] \delta(\sum_{n=1}^{N} \mathbf{p}_n - \mathbf{P}) \, \delta(\sum_{n=1}^{N} \frac{p_n^2}{2m_n} - E) . \tag{D-4}$$

This can be accomplished by the same technique, applied to both δ-functions,

$$\mathcal{I}_N = \int \frac{dt}{h} \exp(\frac{i}{\hbar}Et) \int \frac{d\mathbf{R}}{h^3} \exp(\frac{i}{\hbar}\mathbf{P}\cdot\mathbf{R}) \prod_{n=1}^{N} \left[\int d\mathbf{p}_n \exp[-\frac{i}{\hbar}(\frac{p_n^2}{2m_n}t + \mathbf{p}_n\cdot\mathbf{R})] \right] . \tag{D-5}$$

The part of the exponent containing $\mathbf{p}_n$ can be readily brought on normal form,

$$\frac{p_n^2}{2m_n}t + \mathbf{p}_n\cdot\mathbf{R} = \frac{t}{2m_n}(\mathbf{p}_n + \frac{m_n}{t}\mathbf{R})^2 - \frac{m_n}{2t}R^2 , \tag{D-6}$$

so the integrals over $\mathbf{p}_n$ can be performed,

$$\begin{aligned} \mathcal{I}_N(\mathbf{P},E) &= \int \frac{dt}{h} \exp(\frac{i}{\hbar}Et) \int \frac{d\mathbf{R}}{h^3} \exp(\frac{i}{\hbar}\mathbf{P}\cdot\mathbf{R}) \prod_{n=1}^{N} \left[(\frac{hm_n}{it})^{\frac{3}{2}} \exp(\frac{i}{\hbar}\frac{m_n}{2t}R^2) \right] \\ &= \int \frac{dt}{h} \exp(\frac{i}{\hbar}Et) \prod_{n=1}^{N} \left[\frac{hm_n}{it} \right]^{\frac{3}{2}} \int \frac{d\mathbf{R}}{h^3} \exp[\frac{i}{\hbar}(\mathbf{P}\cdot\mathbf{R} + \frac{m_0}{2t}R^2)] . \end{aligned} \tag{D-7}$$

The part of the exponent depending on $\mathbf{R}$ can then be completed,

$$\frac{m_0}{2t}R^2 + \mathbf{R}\cdot\mathbf{P} = \frac{m_0}{2t}(\mathbf{R} + \frac{t}{m_0}\mathbf{P})^2 - \frac{t}{2m_0}P^2 ; \tag{D-8}$$

and the integrations over $\mathbf{R}$ and t can be carried out,

$$\begin{aligned} \mathcal{I}_N(\mathbf{P},E) &= (\frac{m_1\cdots m_N}{m_0})^{\frac{3}{2}} \int \frac{dt}{h} \exp(\frac{i}{\hbar}Et) \, (\frac{h}{it})^{\frac{3}{2}N-\frac{3}{2}} \\ &= \frac{2\pi}{\Gamma(\frac{3}{2}N-\frac{3}{2})} (\frac{m_1\cdots m_N}{m_0})^{\frac{3}{2}} \left[2\pi(E - \frac{P^2}{2m_0}) \right]^{\frac{3}{2}N-\frac{5}{2}} . \end{aligned} \tag{D-9}$$

Again we have used Hankel's Contour Integral to arrive at the last relation. This result appears also quite plausible, since the requirement of momentum conservation eliminates three more degrees of freedom and also reduces the energy available for random motion by the kinetic energy tied up in the overall translational motion, $P^2/2m_0$.

D.3 Conservation of energy, momentum, and outwards flow

Finally, the most complicated integral needed expresses the phase space for fragment motion when overall energy and momentum conservation is imposed and a specified outwards flow p is required as well,

$$\mathcal{I}_N(\mathbf{P},E,p) \equiv \prod_{n=1}^{N} \left[\int d\mathbf{p}_n \right] \delta(\sum_{n=1}^{N} \mathbf{p}_n - \mathbf{P}) \, \delta(\sum_{n=1}^{N} \frac{p_n^2}{2m_n} - E) \, \delta(\frac{1}{q_0}\sum_{n=1}^{N} \mathbf{p}_n\cdot\mathbf{r}_n - p) . \tag{D-10}$$

Again the Fourier representation of the δ-function can be exploited,

$$\begin{aligned} \mathcal{I}_N(\mathbf{P},E,p) &= \int \frac{dt}{h} \exp(\frac{i}{\hbar}Et) \int \frac{d\mathbf{R}}{h^3} \exp(\frac{i}{\hbar}\mathbf{P}\cdot\mathbf{R}) \int \frac{dq}{h} \exp(\frac{i}{\hbar}pq) \\ &\times \prod_{n=1}^{N} \left[\int d\mathbf{p}_n \exp[-\frac{i}{\hbar}(\frac{p_n^2}{2m_n}t + \mathbf{p}_n\cdot\mathbf{R} + \mathbf{p}_n\cdot\mathbf{q}_n)] \right] , \end{aligned} \tag{D-11}$$

where we have introduced the convenient notation $\mathbf{q}_n \equiv q\hat{\mathbf{r}}_n$. The first step is to bring the exponents on normal form so that the momentum integrals can be performed,

$$\frac{p_n^2}{2m_n}t + \mathbf{p}_n \cdot \mathbf{R} + \mathbf{p}_n \cdot \mathbf{q}_n = \frac{t}{2m_n}(\mathbf{p}_n + \frac{m_n}{t}(\mathbf{R} + \mathbf{q}_n))^2 - \frac{m_n}{2t}(\mathbf{R} + \mathbf{q}_n)^2 \ . \qquad (\mathfrak{D}\text{-}12)$$

We then have

$$\begin{aligned} \mathcal{I}_N(\mathbf{P}, E, p) &= \int \frac{dt}{h} \exp(\frac{i}{\hbar}Et) \int \frac{d\mathbf{R}}{h^3} \exp(\frac{i}{\hbar}\mathbf{P} \cdot \mathbf{R}) \\ &\times \int \frac{dq}{h} \exp(\frac{i}{\hbar}pq) \prod_{n=1}^{N} \left[(\frac{hm_n}{it})^{\frac{3}{2}} \exp[\frac{i}{\hbar}\frac{m_n}{t}(\mathbf{R} + \mathbf{q}_n)^2] \right] \ . \end{aligned} \qquad (\mathfrak{D}\text{-}13)$$

The next step is to perform the q integration and for that the exponent is rewritten as follows,

$$\begin{aligned} pq + \sum_n \frac{m_n}{2t}(\mathbf{R} + \mathbf{q}_n)^2 &= pq + \frac{1}{2t}m_0(R^2 + q^2) \\ &= \frac{m_0}{2t}(q + \frac{t}{m_0}p)^2 - \frac{t}{2m_0}p^2 + \frac{m_0}{2t}R^2 \ . \end{aligned} \qquad (\mathfrak{D}\text{-}14)$$

For simplicity we have here assumed that the overall center of mass is located at the origin, $\sum_n m_n \mathbf{r}_n = \mathbf{0}$, and that $\sum_n m_n r_n^2 = m_0 q_0^2$, as will be the case in our applications. The q-integration can now be performed and we obtain

$$\begin{aligned} \mathcal{I}_N(\mathbf{P}, E, p) &= \int \frac{dt}{h} \exp(\frac{i}{\hbar}Et) \int \frac{d\mathbf{R}}{h^3} \exp(\frac{i}{\hbar}\mathbf{P} \cdot \mathbf{R}) \prod_{n=1}^{N} \left[\frac{m_n h}{it} \right]^{\frac{3}{2}} \\ &\times (\frac{\hbar m_0}{it})^{-\frac{1}{2}} \exp(\frac{i}{\hbar}(\frac{t}{2m_0}p^2 + \frac{m_0}{2t}R^2) \ . \end{aligned} \qquad (\mathfrak{D}\text{-}15)$$

Subsequently, the $\mathbf{R}$-integration can be carried out, using

$$\mathbf{P} \cdot \mathbf{R} + \frac{m_0}{2t}R^2 = \frac{m_0}{2t}(\mathbf{R} + \frac{t}{m_0}\mathbf{P})^2 - \frac{t}{2m_0}P^2 \ , \qquad (\mathfrak{D}\text{-}16)$$

so we are left with an elementary integral over t,

$$\begin{aligned} \mathcal{I}_N(\mathbf{P}, E, p) &= \int \frac{dt}{h} \exp(\frac{i}{\hbar}Et) \prod_{n=1}^{N} \left[\frac{hm_n}{it} \right]^{\frac{3}{2}} (\frac{hm_0}{it})^{-2} \exp[\frac{i}{\hbar}(E - \frac{P^2}{2m_0} - \frac{p^2}{2m_0})t] \\ &= \frac{2\pi}{\Gamma(\frac{3}{2}N - 2)} \frac{(m_1 \cdots m_N)^{\frac{3}{2}}}{m_0^2} \left[2\pi(E - \frac{P^2}{2m_0} - \frac{p^2}{2m_0}) \right]^{\frac{3}{2}N-3} \ . \end{aligned} \qquad (\mathfrak{D}\text{-}17)$$

This result is also easy to accept, since the additional constraint on the outwards flow ties up one more degree of freedom and further reduces the available kinetic energy by the flow energy $p^2/2m_0$.

D.4 Constrained positions

In the present treatment, we need to evaluate the phase space associated with the fragment positions when these are constrained to yield a specified overall center-of-mass position and, at the same time, a specified spatial extension of the system, as given in terms of the disassembly coordinate q of eq. (9),

$$\mathcal{I}_N(\mathbf{R}, q) \equiv \prod_{n=1}^{N} \left[\int d\mathbf{r}_n\right] \; \delta(\frac{1}{m_0}\sum_{n=1}^{N} m_n \mathbf{r}_n - \mathbf{R}) \; 2q\delta(\frac{1}{m_0}\sum_{n=1}^{N} m_n r_n^2 - q^2) \; . \qquad (\mathfrak{D}\text{-}18)$$

The form of this integral is quite similar to the expression ($\mathfrak{D}$-4) for $\mathcal{I}_N(\mathbf{P}, E)$. Indeed, by making the substitutions $\mathbf{p}_n \rightarrow m_n \mathbf{r}_n$ in ($\mathfrak{D}$-4) we readily find that $\mathcal{I}_N(\mathbf{R}, q)$ is equal to $\mathcal{I}_N(\mathbf{P} \rightarrow m_0\mathbf{R}, E \rightarrow \frac{m_0}{2}q^2)$, *i.e.*

$$\mathcal{I}_N(\mathbf{R}, q) = \frac{2\pi}{\Gamma(\frac{3}{2}N - \frac{3}{2})} \; (\frac{m_0}{m_1} \cdots \frac{m_0}{m_N})^{\frac{3}{2}} \; [\pi(q^2 - R^2)]^{\frac{3}{2}N - \frac{5}{2}} q \; . \qquad (\mathfrak{D}\text{-}19)$$

It should be noted that the hypersurface area defined in (15) is given by $\Omega'_N(q) = \mathcal{I}_N(\mathbf{R} = \mathbf{0}, q)$.

E Angular momentum

In the main text of this paper, we have formulated our multifragmentation theory without regard for the conservation of angular momentum. Here we discuss this aspect of the problem and show how angular-momentum conservation can be readily incorporated, with insignificant additional complication.

E.1 Nuclear level density

We first consider the level density for a single nuclear fragment. The standard Fermi-gas level density $\rho(\epsilon)$ given in ($\mathfrak{B}$-1) has been derived by considering all possible many-particle excitations compatible with the specified constraint on the total energy.[15] This procedure includes all excited nuclear states having an energy ϵ in the specified interval, irrespective of their angular momentum $\mathbf{S}$. Since the disassembling system is isolated, its total angular momentum remains constant, and so we need the density of states having a specified angular momentum, $\rho_{\mathbf{S}}(\epsilon)$. We are particularly interested in the density of states corresponding to a vanishing angular momentum, $\rho_0(\epsilon)$. This quantity is often denoted the *intrinsic* level density, since it is the level density seen by an observer in a body-fixed frame. The density of states for a finite angular momentum can be readily obtained in terms of the intrinsic level density as[16]

$$\rho_{\mathbf{S}}(\epsilon) \; = \; \rho_0(\epsilon - \frac{S^2}{2\mathcal{I}}) \; \approx \; \rho_0(\epsilon) \; e^{-S^2/2\mathcal{I}\tau} \; . \qquad (\mathfrak{E}\text{-}1)$$

Here $\mathcal{I} \approx \frac{1}{5}mR^2$ is the moment of inertia and $S^2/2\mathcal{I}$ represents the energy associated with the overall rotation of the system. This quantity must be subtracted from the

specified total energy ϵ in order to obtain the energy available for intrinsic nuclear excitation. The second, approximate relation follows by performing a logarithmic expansion of the level density, with the temperature given by $1/\tau = \partial \ln \rho / \partial \epsilon$, as usual.

From the above relation it is now easy to calculate the total level density $\rho(\epsilon)$, on which no restriction on $\mathbf{S}$ has been imposed. It can be obtained by simply adding the contributions from all values of $\mathbf{S}$,

$$\begin{aligned} \rho(\epsilon) &= 8\pi^2 \int \frac{d\mathbf{S}}{h^3}\, \rho_{\mathbf{S}}(\epsilon) \approx \rho_0(\epsilon)\, \frac{8\pi^2}{h^3} \int d\mathbf{S}\; \mathrm{e}^{-S^2/2\mathcal{I}\tau} \\ &= \frac{8\pi^2}{h^3}(2\pi\mathcal{I}\tau)^{\frac{3}{2}}\; \rho_0(\epsilon) = \zeta_{\mathrm{rot}}(\tau)\; \rho_0(\epsilon)\;. \end{aligned} \tag{E-2}$$

The factor $8\pi^2$ arises from the integration over all possible orientations of the rotor, as specified by the three Euler angles (θ, ϕ, ψ). [The angles (θ, ϕ) specify the direction of the major axis, and thus span a solid angle of 4π, while the third angle ψ specifies the additional rotation of the body around its major axis, and thus has a range of 2π.]

The above result (E-2) shows that the unrestricted level density for the rotating nucleus, $\rho(\epsilon)$, is simply equal to that for the static one, $\rho_0(\epsilon)$ multiplied by the partition function $\zeta_{\mathrm{rot}}(\tau)$ associated with the overall rotation. Being a specific instance of a more general feature, the above result is accurate when the amount of energy associated with the overall rotation, $S^2/2\mathcal{I}$, forms only a small fraction of the total energy ϵ, so that the values of $\mathbf{S}$ have a canonical distribution. The result can be used to find the intrinsic level density $\rho_0(\epsilon)$ in terms of the unrestricted level density $\rho(\epsilon)$, $\rho_0(\epsilon) = \rho(\epsilon)/\zeta_{\mathrm{rot}}(\tau)$. Furthermore, invoking (E-1), the nuclear level density for a specified value of $\mathbf{S}$ can be written as

$$\rho_{\mathbf{S}}(\epsilon) \approx \frac{h^3}{8\pi^2}(2\pi\mathcal{I}\tau)^{-\frac{3}{2}}\; \rho(\epsilon - S^2/2\mathcal{I}) \;\approx \frac{h^3}{8\pi^2}(2\pi\mathcal{I}\tau)^{-\frac{3}{2}}\; \mathrm{e}^{-S^2/2\mathcal{I}\tau}\; \rho(\epsilon - S^2/2\mathcal{I})\;. \tag{E-3}$$

E.2 Multifragment system

The above method is quite general and can be applied to the density of states for the multifragment system as well. Thus, when the additional demand of a constant angular momentum is imposed, the density of states (16) for the multifragment system is modified to

$$\begin{aligned} &\frac{h^3}{8\pi^2}\, h^3\, \frac{dN_{A_1\cdots A_N}(E)}{d\mathbf{J}d\mathbf{R}d\mathbf{P}dE} \approx \\ &\langle\, \frac{2}{\Gamma(\frac{3}{2}N - \frac{3}{2})} \int \frac{dq}{q}\, \frac{1}{\zeta_{1\cdots N}(\bar{\tau})}\, (\frac{m_0 q^2 \bar{\tau}}{2\hbar^2})^{\frac{3}{2}N - \frac{3}{2}}\; \rho_{1\cdots N}(\epsilon'_{1\cdots N})\, \rangle'\;. \end{aligned} \tag{E-4}$$

Here $\epsilon'_{1\cdots N} = \epsilon_{1\cdots N} - J^2/2\mathcal{I}_{1\cdots N}$ is the statistical part of the excitation energy and

$$\zeta_{1\cdots N}(\bar{\tau}) = \frac{8\pi^2}{h^3}(2\pi\mathcal{I}_{1\cdots N}\bar{\tau})^{\frac{3}{2}} \tag{E-5}$$

is the rotational partition function associated with the particular spatial configuration of the multifragment system. The effective moment of inertia $\mathcal{I}_{1\ldots N}$ is the cube root of the determinant of the corresponding inertial tensor, $\mathcal{I}^3_{1\ldots N} = |\overleftrightarrow{\mathcal{I}}_{1\ldots N}|$, with

$$\overleftrightarrow{\mathcal{I}}_{1\ldots N} = \sum_{n=1}^{N} (\overleftarrow{r_n}\, m_n\, \overrightarrow{r_n} + \mathcal{I}_n\, \overleftrightarrow{1}) \,, \tag{E-6}$$

where $\overleftrightarrow{1}$ is the unit 3×3 tensor and $\mathcal{I}_n$ is the moment of inertia for fragment n.

It is thus straightforward to incorporate conservation of angular momentum into the density of states $\rho(A, E)$ for the decaying compound system. At not too extreme excitations, the dominant contribution in the multifragment expansion (6) for $\rho(A, E)$ is the mononuclear term $\rho_A(\epsilon_0)$. If only this term is considered, the angular-momentum conserving compound nuclear level density becomes

$$\rho(A, E, \mathbf{J}) = \frac{h^3}{8\pi}(2\pi\mathcal{I}_A\tau_0)^{-\frac{3}{2}}\, \rho_A(\epsilon_0') \,, \tag{E-7}$$

where $\mathcal{I}_A$ is the moment of inertia of the compound nucleus, τ_0 is its temperature, and $\rho_A(\epsilon_0)$ is the Fermi-gas level density given in (B-1). The argument in the unrestricted level density is the reduced, intrinsic excitation energy $\epsilon_0' = \epsilon_0 - J^2/2\mathcal{I}_A$.

The incorporation of angular-momentum conservation into the expression for the transition current $\nu_{A_1\ldots A_N}(E)$ can be made in the same manner. When the effect is also included in the compound level density as described above, the expression for the transition width becomes

$$\Gamma_{A_1\ldots A_N}(E, \mathbf{J}) \approx \frac{1}{\rho_A(\epsilon_0')} \frac{\sqrt{4\pi}}{\Gamma(\frac{3}{2}N - \frac{3}{2})} \left\langle \left(\frac{\mathcal{I}_A\tau_0}{\mathcal{I}_{1\ldots N}\bar{\tau}}\right)^{\frac{3}{2}} \left(\frac{m_0 q^2_{1\ldots N}\bar{\tau}}{2\hbar^2}\right)^{\frac{3}{2}N-2} \rho_{1\ldots N}(\epsilon'_{1\ldots N})\, \bar{\tau} \right\rangle' , \tag{E-8}$$

where the argument in the level density is the intrinsic excitation $\epsilon'_{1\ldots N} = \epsilon_{1\ldots N} - J^2/2\mathcal{I}_{1\ldots N}$. Thus the resulting expression is very similar to the one given in (20) which was derived without considering the angular momentum. The effect of this refinement is not very large, because it affects the transition current in the numerator and the compound level density in the denominator in qualitatively the same manner.

It is instructive to extend our formulation to take explicit account of angular momentum. The density of states for a specified total angular momentum $\mathbf{J}$ is given by

$$\frac{dN_{A_1\ldots A_N}(E)}{d\mathbf{J}\, d\mathbf{R}\, d\mathbf{P}\, dE} = \tag{E-9}$$
$$\prod_{n=1}^{N} \left[\int \frac{d\mathbf{r}_n d\mathbf{p}_n}{h^3} \int \frac{d\mathbf{S}_n}{\pi\hbar^3} \int d\epsilon_n \rho_n^0(\epsilon_n) \right] \delta(E_F - E)\, \delta(\mathbf{R}_F)\delta(\mathbf{P}_F)\, \delta(\mathbf{J}_F - \mathbf{J}) \,.$$

Here $\rho_n^0(\epsilon_n)$ denotes the intrinsic level density for the fragment n and $\mathbf{S}_n$ is its angular momentum. The total angular momentum of the multifragment system is

given by

$$\mathbf{J}_F = \sum_{n=1}^{N} (\mathbf{r}_n \times \mathbf{p}_n + \mathbf{S}_n) \tag{E-10}$$

and the energy of a given fragmentation now includes explicitly the rotational energy,

$$E_F = E^0_{1\ldots N} + V + \sum_{n=1}^{N} (\frac{p_n^2}{2m_n} + \frac{S_n^2}{2\mathcal{I}_n} + \epsilon_n) \ . \tag{E-11}$$

The integrals over the fragment spins can be readily carried out by exploiting their analogy with the constrained momentum integrals in Section D.2 However, this operation leaves an expression which is generally impossible to evaluate exactly.

E.3 Binary system

It is instructive to consider in some detail the case of $N = 2$ and $\mathbf{J} = \mathbf{0}$, for which the above exact expression (E-9) can be easily evaluated.

The first step is to change variables from those describing the individual fragments, $(\mathbf{r}_1, \mathbf{p}_1)$ and $(\mathbf{r}_2, \mathbf{p}_2)$, to those associated with the overall CM system, $(\mathbf{R}, \mathbf{P})$, and the relative motion, $(\mathbf{r}_{12}, \mathbf{p}_{12})$. The integration over the former ones then eliminates the constraints on $\mathbf{R}_F$ and $\mathbf{P}_F$.

Subsequently, the constrained integration over the fragment spins $\mathbf{S}_1$ and $\mathbf{S}_2$ can be carried out utilizing (D-9), as explained above. Furthermore, the relationship (E-1) may be exploited to replace the intrinsic level densities $\rho^0_n(\epsilon_n)$ by the standard unconstrained level densities $\rho_n(\epsilon_n)$ which are more convenient; this replacement yields a factor of ζ_n^{-1} for each fragment. After these manipulations are carried out, we obtain

$$\frac{h^3}{8\pi^2}\, h^3\, \frac{dN_{A_1A_2}(E)}{d\mathbf{J}d\mathbf{R}d\mathbf{P}dE} = \frac{1}{\Gamma(\frac{3}{2})}\frac{h^3}{8\pi^2}[2\pi(\mathcal{I}_1+\mathcal{I}_2)\bar{\tau}^2]^{-\frac{3}{2}} \tag{E-12}$$

$$\times \int \frac{d\mathbf{r}_{12}d\mathbf{p}_{12}}{h^3} \int d\epsilon\, \rho_{12}(\epsilon) \left[E - E^0_{12} - V - \epsilon - \frac{p_{12}^2}{2\mu} - \frac{(\mathbf{r}_{12}\times\mathbf{p}_{12})^2}{2(\mathcal{I}_1+\mathcal{I}_2)}\right]^{\frac{1}{2}} \ .$$

In order to proceed, we note that $(\mathbf{r}_{12} \times \mathbf{p}_{12})^2 = r_{12}^2 p_t^2$, where p_t is magnitude of the tangential component of the relative momentum $\mathbf{p}_{12}$; the relative radial momentum is given by $p_r = \mathbf{p}_{12} \cdot \hat{\mathbf{r}}_{12}$. Since $d\mathbf{R}_{12} = \pi dp_t^2 dp_r$, the integration over p_t can be readily carried out. In order to obtain the final result, we note that $\mu r_{12}^2 = m_0 q^2$ and $p_r^2/2\mu = p^2/2m_0 = k$, where q and p are the disassembly variables (9-10).

The transition current can be calculated in the same manner, leading to

$$\nu_{A_1A_2}(E, \mathbf{J}=\mathbf{0}) \approx \left[\frac{8\pi^2}{h^3}(2\pi\mathcal{I}_{12}\bar{\tau})^{\frac{3}{2}}\right]^{-1} \frac{2m_0 q^2 \bar{\tau}}{\hbar^2}\, \rho_{12}(\epsilon_{12})\bar{\tau} \ . \tag{E-13}$$

Here we have also used the approximation (B-8) to carry out the final integration

over the intrinsic excitation energy ϵ. For the disphere the effective moment of inertia $\mathcal{I}_{12}$ is given by

$$\mathcal{I}_{12}^3 = (\mathcal{I}_1 + \mathcal{I}_2)\,(m_0 q^2 + \mathcal{I}_1 + \mathcal{I}_2)^2\,. \tag{E-14}$$

The first factor arises from rotations around the dinuclear axis $\hat{\mathbf{r}}_{12}$, while the last factor is associated with rotations perpendicular to that direction. We observe that the above result is identical to that resulting from the direct application of the simple formula (E-2), which yields $\nu_{A_1A_2}(E, \mathbf{J} = \mathbf{0}) = \nu_{A_1A_N}(E)/\zeta_{\rm rot}$.

References

[1] S.E. Koonin and J. Randrup, Nucl. Phys. **A356** (1981) 223

[2] S.E. Koonin and J. Randrup, Nucl. Phys. **A474** (1987) 173

[3] D.H.E. Gross, Phys. Lett. **161B** (1985) 47; D.H.E. Gross, Zhang Xiao-ze, and Xu Shu-yan, Phys. Rev. Lett. **56** (1986) 1544

[4] J.P. Bondorf, R. Donangelo, I.N. Mishustin, C.J. Pethick, and H. Schulz, Nucl. Phys. **A443** (1985) 321; J.P. Bondorf, R. Donangelo, I.N. Mishustin, and H. Schulz, Nucl. Phys. **A444** (1985) 460

[5] N. Bohr and J.A. Wheeler, Phys. Rev. **56** (1939) 426

[6] W.J. Świątecki, Aust. J. Phys., **36** (1983) 641

[7] J.A. López and J. Randrup, LBL-26810 (1989), in preparation

[8] W.D. Myers and W.J. Świątecki, Lysekil mass formula

[9] W.J. Świątecki, private communication (1988)

[10] W.J. Świątecki, Phys. Scrip. **24** (1981) 113

[11] H.J. Krappe, J.R. Nix, and A.J. Sierk, Phys. Rev. **C20** (1979) 992

[12] A.J. Sierk, LANL Report LA-UR-85-1660 (1985)

[13] J.A. López and J. Randrup, Nucl. Phys. **A491** (1989) 477

[14] M. Abramowitz and I.A. Stegun, *Handbook of Mathematical Functions*, Dover Publications (New York) 1970

[15] A. Bohr and B.R. Mottelson, *Nuclear Structure I*, Benjamin, (New York) 1969

[16] S. Bjørnholm, A. Bohr, and B.R. Mottelson, Third IAEA Symposium on the Physics and Chemistry of Fission, Rochester, New York (1973) 367

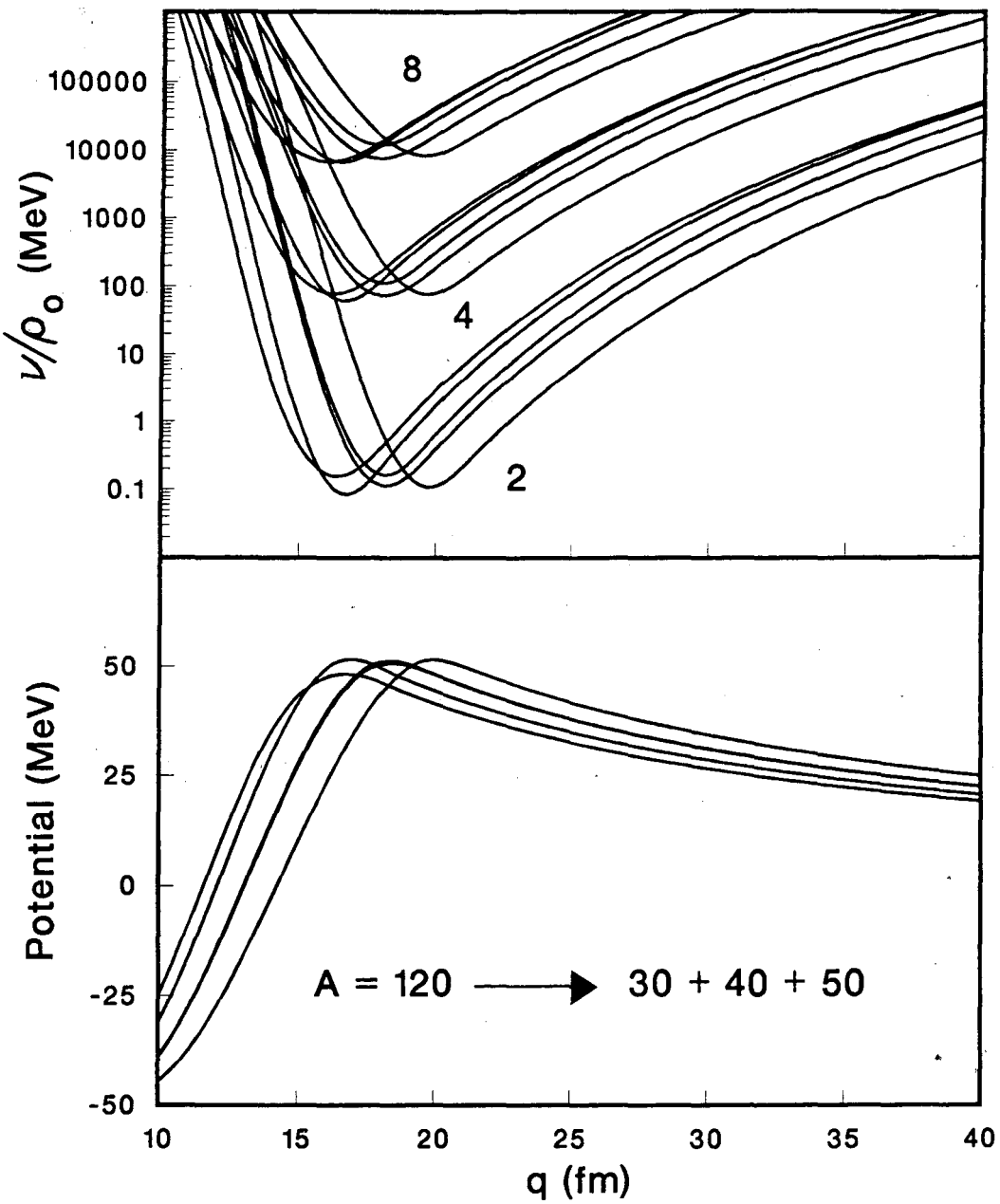

Figure 1: Transition current

Lower portion: The potential energy V_{123} as a function of the *rms* extension q for a random sample of 5 ternary splits of ^{120}Sn into the mass partition $30 + 40 + 50$. *Upper portion:* For the excitation energies $\epsilon_0 = E_0^\star = 2, 4, 8$ MeV per nucleon, the associated outwards currents $\nu_{123}(E)$ are shown as functions of q. For convenience, the currents have been divided by the mononuclear level density $\rho_0(E_0^\star)$. The global minima in these curves identify the location $q = q_{123}$ of the respective transition configurations, and the corresponding value of the ratio ν_{123}/ρ_0 is the contribution to the breakup width $\Gamma_{123}(E)$ from that particular configuration.

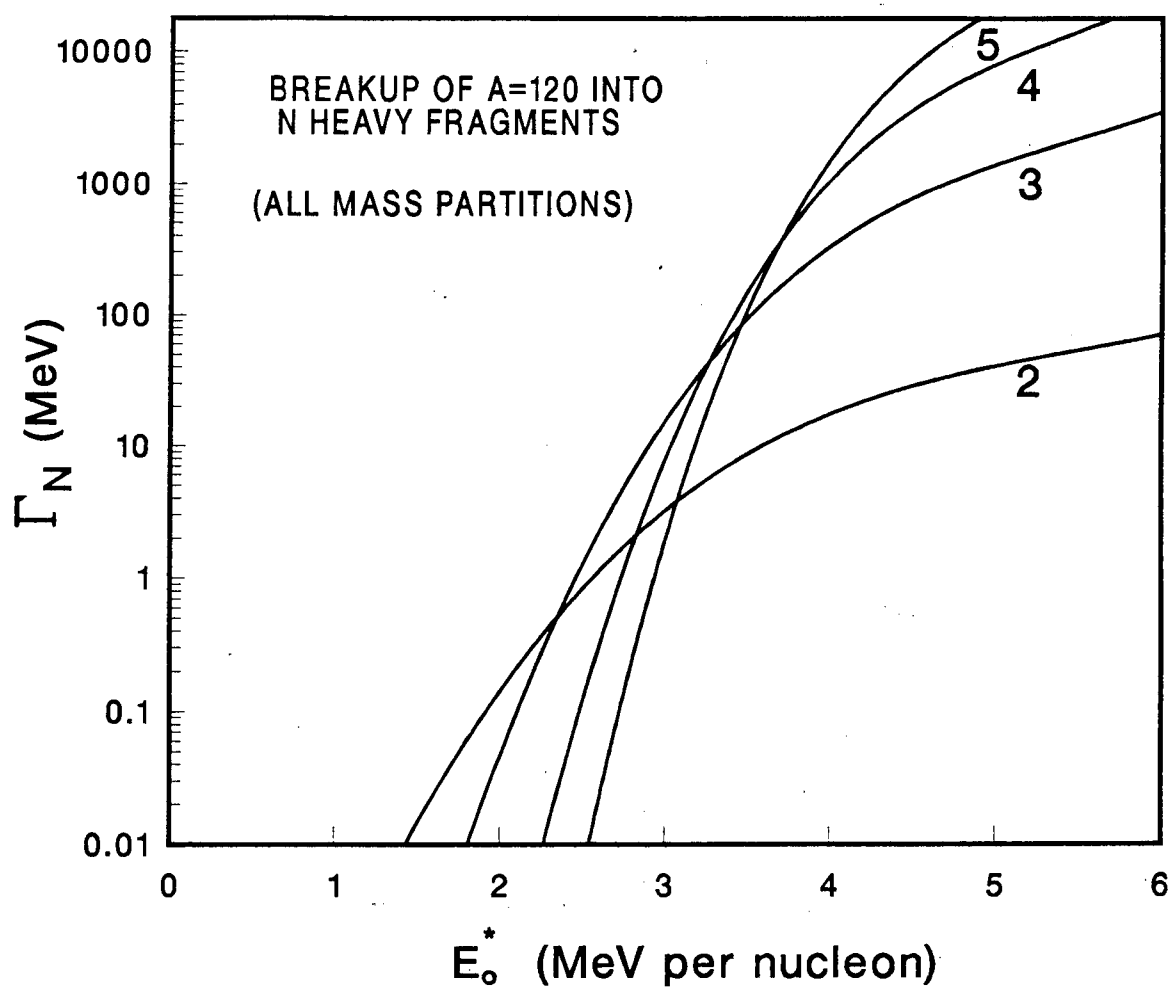

Figure 2: Partial width for breakup into N prefragments
The partial widths $\Gamma_A^N(E)$ (see eq. 20) for breakup of ^{120}Sn into N fragments with mass numbers $A > 10$ are shown as functions of the excitation energy $E_0^\star = E - E_0$ in the source (also denoted by ϵ_0). The curves are labelled by the value of N.

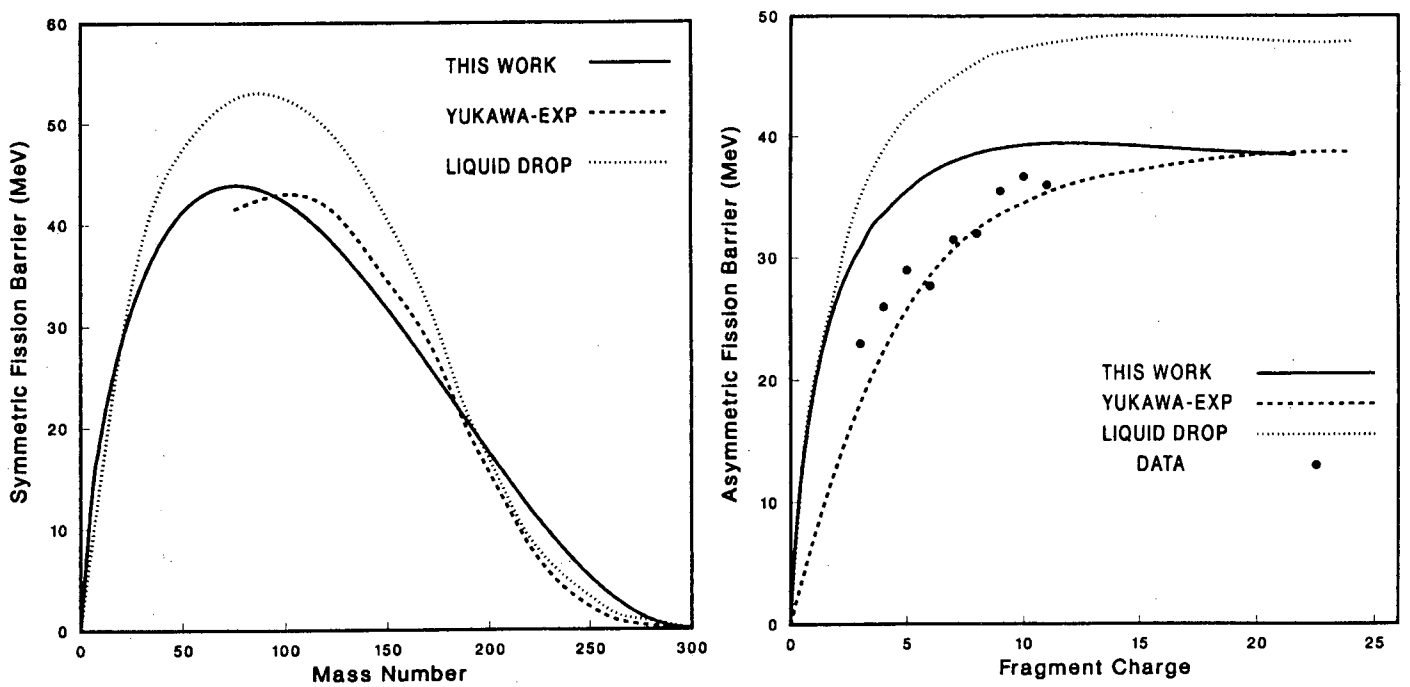

Figure 3: Fission barriers heights

LHS: Symmetric fission barrier heights for nuclei along the line of β stability calculated with the liquid drop model (dots) and the Yukawa-plus-exponential model (dashes) (from [11]). The modified Swiatecki parametrization ($\mathbf{A}$-6) adopted in the present work is shown by the solid curve [9].

RHS: Asymmetric fission barrier heights for $^{110-112}$In, as obtained in ref. [12] with the liquid-drop model (dots) and the Yukawa-plus-exponential model (dashes). The solid curve is our adopted parametrization[9] and the solid dots indicate experimental data (also taken from ref. [12]).

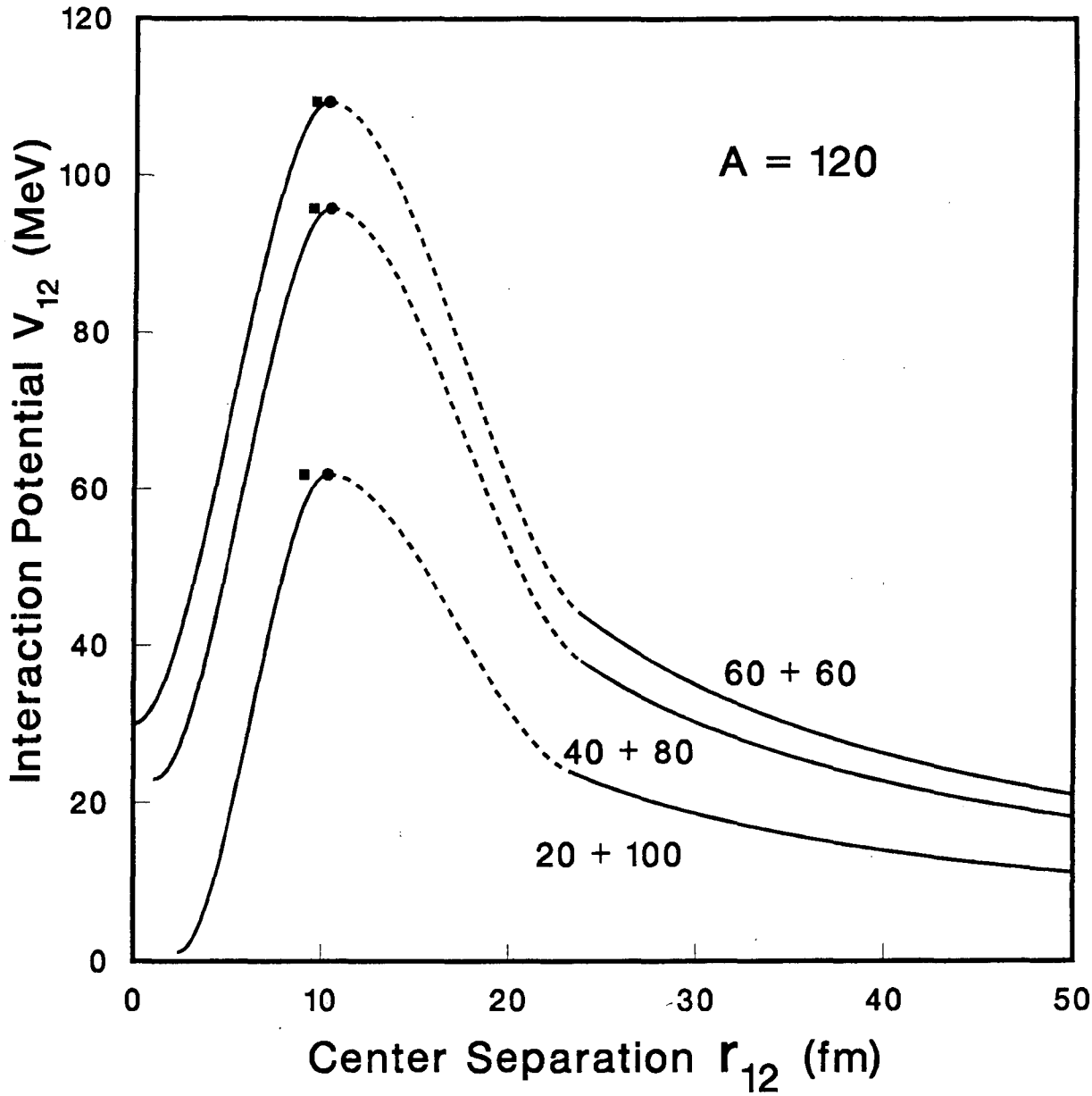

Figure 4: Prefragment interaction potential
The interaction potential V_{12} between two prefragments as a function of their center separation coordinate r_{12}, for three mass asymmetric splits of the nucleus ^{120}Sn. The different sections of the curves correspond to the three regions of the center separation $r_{12} = |\mathbf{r}_1 - \mathbf{r}_2|$. The solid circle shows the location of the saddle point and the solid square corresponds to a touching configuration of the two spheres. The interaction potential is defined such that it tends to zero for large separations.

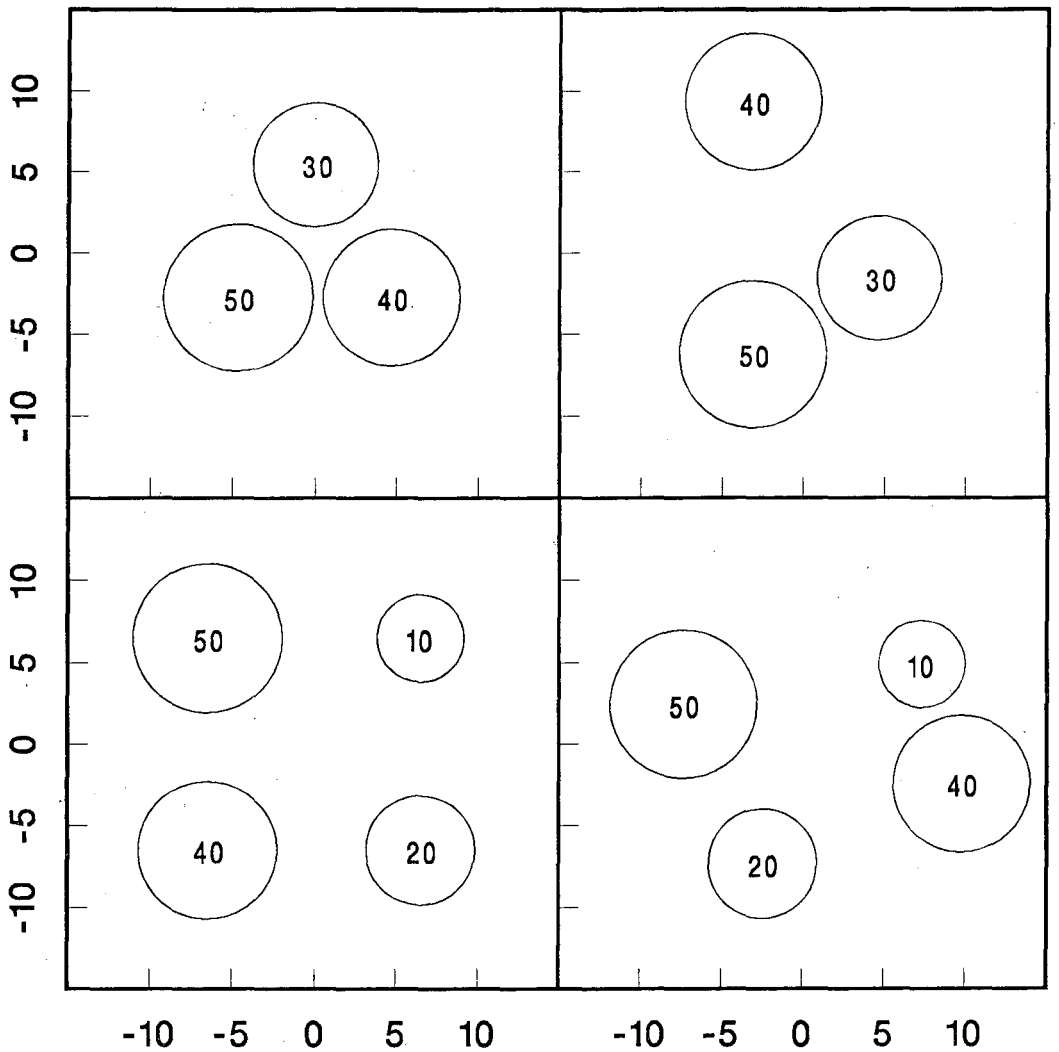

Figure 5: Transition configurations
Some transition configurations for breakup of ^{120}Sn into either three (top) or four (bottom) fragments, with masses as indicated. The four fragments have been chosen to lie in the same plane (the three fragments always do). The figure illustrates how well developed the prefragments typically are in the transition configurations.

LAWRENCE BERKELEY LABORATORY
TECHNICAL INFORMATION DEPARTMENT
1 CYCLOTRON ROAD
BERKELEY, CALIFORNIA 94720